Publish Date:
February 2017
Volume 3, Issue 1

JSHD

Journal of Structural Heart Disease

OFFICIAL JOURNAL OF THE PICS FOUNDATION

PICS Foundation

PEDIATRIC AND ADULT INTERVENTIONAL CARDIAC SYMPOSIUM

Published by
Science International Corp.
ISSN 2325-4637

Now accepting papers at http://structuralheartdisease.org

Committed to Advancing Transcatheter Heart Valve Therapy

Edwards SAPIEN XT Transcatheter Heart Valve

Approved for Pulmonic Procedures

The SAPIEN XT valve is approved for pulmonic procedures in pediatric and adult patients with a dysfunctional, non-compliant right ventricular outflow tract (RVOT) conduit.

SAPIEN XT Valve Sizing—Pulmonic

23 mm	26 mm	29 mm
20-23 mm	23-26 mm	26-29 mm

Diameter of intended location within the conduit

Edwards Lifesciences is driving the innovation, collaboration, and education needed to bring transcatheter technology to more patients worldwide.

» Visit **Edwards.com/pulmonic** for more information

See adjacent page for Important Safety Information.

CAUTION: Federal (United States) law restricts this device to sale by or on the order of a physician.

Edwards Lifesciences • One Edwards Way, Irvine CA 92614 USA • edwards.com

Edwards

Important Safety Information

EDWARDS SAPIEN XT TRANSCATHETER HEART VALVE WITH THE NOVAFLEX+ DELIVERY SYSTEM – PULMONIC

Indications: The Edwards SAPIEN XT transcatheter heart valve (THV) systems are indicated for use in pediatric and adult patients with a dysfunctional, non-compliant right ventricular outflow tract (RVOT) conduit with a clinical indication for intervention and: pulmonary regurgitation ≥ moderate and/or mean RVOT gradient ≥ 35 mmHg.

Contraindications: The THV and delivery systems are contraindicated in patients with inability to tolerate an anticoagulation/antiplatelet regimen or who have active bacterial endocarditis.

Warnings: The devices are designed, intended, and distributed for single use only. **Do not resterilize or reuse the devices.** There are no data to support the sterility, nonpyrogenicity, and functionality of the devices after reprocessing. Assessment for coronary compression risk prior to valve implantation is essential to prevent the risk of severe patient harm. Incorrect sizing of the THV may lead to paravalvular leak, migration, embolization and/or RVOT rupture. Accelerated deterioration of the THV may occur in patients with an altered calcium metabolism. Prior to delivery, the THV must remain hydrated at all times and cannot be exposed to solutions other than its shipping storage solution and sterile physiologic rinsing solution. THV leaflets mishandled or damaged during any part of the procedure will require replacement of the THV. Do not use the THV if the tamper evident seal is broken, the storage solution does not completely cover the THV, the temperature indicator has been activated, the THV is damaged, or the expiration date has elapsed. Do not mishandle the NovaFlex+ delivery system or use it if the packaging or any components are not sterile, have been opened or are damaged (e.g. kinked or stretched), or the expiration date has elapsed. Use of excessive contrast media may lead to renal failure. Measure the patient's creatinine level prior to the procedure. Contrast media usage should be monitored. Patient injury could occur if the delivery system is not un-flexed prior to removal. Care should be exercised in patients with hypersensitivities to cobalt, nickel, chromium, molybdenum, titanium, manganese, silicon, and/or polymeric materials. The procedure should be conducted under fluoroscopic guidance. Some fluoroscopically guided procedures are associated with a risk of radiation injury to the skin. These injuries may be painful, disfiguring, and long-lasting. THV recipients should be maintained on anticoagulant/antiplatelet therapy as determined by their physician. This device has not been tested for use without anticoagulation. Do not add or apply antibiotics to the storage solution, rinse solutions, or to the THV.

Precautions: Safety, effectiveness, and durability of the THV have not been established for implantation within a previously placed surgical or transcatheter pulmonic valve. Long-term durability has not been established for the THV. Regular medical follow-up is advised to evaluate THV performance. Glutaraldehyde may cause irritation of the skin, eyes, nose and throat. Avoid prolonged or repeated exposure to, or breathing of, the solution. Use only with adequate ventilation. If skin contact occurs, immediately flush the affected area with water; in the event of contact with eyes, immediately flush the affected area with water and seek immediate medical attention. For more information about glutaraldehyde exposure, refer to the Material Safety Data Sheet available from Edwards Lifesciences. Patient anatomy should be evaluated to prevent the risk of access that would preclude the delivery and deployment of the device. To maintain proper valve leaflet coaptation, do not overinflate the deployment balloon. Appropriate antibiotic prophylaxis is recommended post-procedure in patients at risk for prosthetic valve infection and endocarditis. Safety and effectiveness have not been established for patients with the following characteristics/comorbidities: Echocardiographic evidence of intracardiac mass, thrombus, or vegetation; a known hypersensitivity or contraindication to aspirin, heparin or sensitivity to contrast media, which cannot be adequately premedicated; pregnancy; and patients under the age of 10 years.

Potential Adverse Events: Potential risks associated with the overall procedure including potential access complications associated with standard cardiac catheterization, balloon valvuloplasty, the potential risks of conscious sedation and/or general anesthesia, and the use of angiography: death; respiratory insufficiency or respiratory failure; hemorrhage requiring transfusion or intervention; cardiovascular injury including perforation or dissection of vessels, ventricle, myocardium or valvular structures that may require intervention; pericardial effusion or cardiac tamponade; embolization including air, calcific valve material or thrombus; infection including septicemia and endocarditis; heart failure; myocardial infarction; renal insufficiency or renal failure; conduction system defect arrhythmia; arteriovenous fistula; reoperation or reintervention; ischemia or nerve injury; pulmonary edema; pleural effusion, bleeding; anemia; abnormal lab values (including electrolyte imbalance); hypertension or hypotension; allergic reaction to anesthesia, contrast media, or device materials; hematoma or ecchymosis; syncope; pain or changes at the access site; exercise intolerance or weakness; inflammation; angina; fever. Additional potential risks associated with the use of the THV, delivery system, and/or accessories include: cardiac arrest; cardiogenic shock; emergency cardiac surgery; coronary flow obstruction/transvalvular flow disturbance; device thrombosis requiring intervention; valve thrombosis; device embolization; device malposition requiring intervention; valve deployment in unintended location; structural valve deterioration (wear, fracture, calcification, leaflet tear/tearing from the stent posts, leaflet retraction, suture line disruption of components of a prosthetic valve, thickening, stenosis); paravalvular or transvalvular leak; valve regurgitation; hemolysis; device explants; nonstructural dysfunction; and mechanical failure of delivery system, and/or accessories.

Edwards Crimper

Indications: The Edwards crimper is indicated for use in preparing the Edwards SAPIEN XT transcatheter heart valve for implantation.

Contraindications: No known contraindications.

Warnings: The device is designed, intended, and distributed for single use only. **Do not resterilize or reuse the device.** There are no data to support the sterility, nonpyrogenicity, and functionality of the device after reprocessing. Do not mishandle the device. Do not use the device if the packaging or any components are not sterile, have been opened or are damaged, or the expiration date has elapsed.

Precautions: For special considerations associated with the use of this device prior to THV implantation, refer to the SAPIEN XT transcatheter heart valve Instructions for Use.

Potential Adverse Events: No known potential adverse events.

CAUTION: Federal (United States) law restricts this device to sale by or on the order of a physician.

Edwards Lifesciences • One Edwards Way, Irvine CA 92614 USA • edwards.com

Edwards

Editorial Board

William E. Hellenbrand	Yale University (New Haven, CT)
James Hermiller	The Care Group (Indianapolis, IN)
Howard Herrmann	University of Pennsylvania (Philadelphia, PA)
David Holmes	Mayo Clinic (Rochester, MN)
Noa Holoshitz	Rush University Medical Center (Chicago, IL)
Ralf Holzer	Sidra Medical & Research Center (Doha, Qatar)
Eric Horlick	University of Toronto (Toronto, Canada)
Reda Ibrahim	Montreal Heart Institute (Montreal, Canada)
Michel Ilbawi	Rush University Medical Center (Chicago, IL)
Frank Ing	LA Children's Hospital (Los Angeles, CA)
Alexander Javois	Hope Children's Hospital (Oak Lawn, IL)
Thomas Jones	Seattle Children's Hospital (Seattle, WA)
Saibal Kar	Cedars Sinai Medical Center (Los Angeles, CA)
Clifford Kavinsky	Rush University Medical Center (Chicago, IL)
Joseph Kay	University of Colorado (Denver, CO)
Damien Kenny	Rush University Medical Center (Chicago, IL)
Morton Kern	University of California Irvine (Irvine, CA)
Michael Kim	University of Colorado (Aurora, CO)
Seong-Ho Kim	Cheju Halla General Hospital (South Korea)
Susheel Kodali	Columbia University Medical Center (New York, NY)
Jackie Kreutzer	Pittsburgh Children's Hospital (Pittsburgh, PA)
Shelby Kutty	Children's Hospital and University of Nebraska Medical Center (Omaha, NB)
Bray Patrick-Lake	PFO Research Foundation (Boulder, CO)
Michael Landzberg	Boston Children's Hospital (Boston, MA)
Geoffrey Lane	Royal Melbourne Hospital (Melbourne, Australia)
Roberto Lang	University of Chicago Medical Center (Chicago, IL)
John Lasala	Barnes Jewish Hospital, Washington University (St. Louis, MO)
Martin B. Leon	Columbia University (New York, NY)
Daniel Levi	UCLA Medical Center (Los Angeles, CA)
Scott Lim	University of Virginia Health System (Charlottesville, VA)
Michael Mack	Baylor Healthcare System (Plano, TX)
Francesco Maisano	University of Zurich (Zurich, Switzerland)
Raj Makkar	Cedars Sinai Medical Center (Los Angeles, CA)
Robert March	Rush University Medical Center (Chicago, IL)
Gwen Mayes	VP National Patient Advocate Foundation (Washington, DC)
Pat McCarthy	Northwestern Memorial Hospital (Chicago, IL)
Doff McElhinney	New York University (New York, NY)
John Messenger	University of Colorado (Denver, CO)
Friedrich Mohr	Herzzentrum Universitaet Leipzig (Leipzig, Germany)
Tarek Momenah	Prince Salman Cardiac Center (Riyadh, Saudi Arabia)
Issam Moussa	(Jacksonville, FL)
Michael Mullen	The Heart Hospital (London, England)
David Muller	St. Vincent's Hospital (Sydney, Australia)
William O'Neill	Henry Ford Hospital (Detroit, MI)
Igor Palacios	Mass General Hospital (Boston, MA)
SJ Park	University of Ulsan College of Medicine (Seoul, Korea)
Carlos Pedra	Danta Pazzanese Instituto de Cardiologia (Sao Paolo, Brazil)
Alejandro Peirone	Children's Hospital of Cordoba (Cordoba, Argentina)
Giacomo Pongiglione	Bambino Gesu Hospital (Rome, Italy)
Matthew Price	Scripps Clinic (La Jolla, CA)
Robert Quaife	University of Colorado (Denver, CO)
Shakeel Qureshi	Evelina Children's Hospital (London, UK)

Steve Ramee	Oschner Clinic (New Orleans, LA)
Mark Reisman	Swedish Medical Center (Seattle, WA)
John Rhodes	Miami Children's Hopsital (Miami, FL)
Charanjit Rihal	Mayo Clinic (Rochester, MN)
Richard Ringel	Johns Hopkins Medical Center (Baltimore, MD)
Carlos Ruiz	Lenox Hill Hospital (New York, NY)
Ernesto Salcedo	University of Colorado (Denver, CO)
Joachim Schofer	Hamburg University Cardiovascular Center (Hamburg, Germany)
Paul Sorajja	Minneapolis Heart Institute Foundation (Minneapolis, MN)
Christian Spies	Queen's Heart Physician Practice (Honolulu, HI)
Frank Silvestry	University of Pennsylvania Hospital (Philadelphia, PA)
Gregg Stone	Columbia University (New York, NY)
Corrado Tamborino	University of Catania (Catania, Italy)
Vinod Thourani	Emory University (Atlanta, GA)
Jonathan Tobis	UCLA Medical Center (Los Angeles, CA)
Murat Tuczu	Cleveland Clinic Foundation (Cleveland, OH)
Zoltan Turi	Robert Wood Johnson Medical School (Camden, NJ)
Alec Vahanian	Bichat University Hospital (Paris, France)
Joseph J. Vettukattil	Spectrum Health (Grand Rapids, MI)
Kevin Walsh	Our Lady's Hospital (Dublin, Ireland)
John Webb	St. Paul Hospital Vancouver (British Columbia, Canada)
Brian Whisenant	Intermountain Medical Center (Salt Lake City, Utah)
Matthew Williams	Mount Sinai Medical Center (New York, NY)
Neil Wilson	University of Colorado (Denver, CO)
Evan Zahn	Cedars Sinai Medical Center (Los Angeles, CA)

JSHD
Journal of Structural Heart Disease

Volume 3, Issue 1, February 2017

Original Scientific Articles

Case Report

Journal of Structural Heart Disease (ISSN 2325-4637) is an online open-access journal issued bi-monthly (6 issues per year, one volume per year) by Science International Corporation.

All correspondence should be directed to: Ziyad M. Hijazi, MD, Editor-in-Chief, Journal of Structural Heart Disease, PO Box 26999, Doha, Qatar. Tel.: +974-4003-6601, E-Mail: jshd@scienceinternational.org

All inquiries regarding copyrighted material from this publication should be directed to Science International Corporation: 70 Forest Street, Suite 6-C, Stamford, CT, 06901, USA. Tel.: +1-203-329-8842, Fax: +1-203-329-8846, E-Mail: skorn@scienceinternational.org

JSHD
Journal of Structural Heart Disease

Original Scientific Article

Journal of Structural Heart Disease, February 2017,
Volume 3, Issue 1:1-7
DOI: http://dx.doi.org/10.12945/j.jshd.2017.16.002

Received: March 25, 2016
Accepted: June 8, 2016
Published online: February 2017

The Occlutech Duct Occluder for Patent Ductus Arteriosus

A Retrospective Case Series

Najib Hanna, MD[1], Ramy Charbel, MD[2*], Ghassan Chehab, MD[1], Bernard Gerbaka, MD[2], Zakhia Saliba, MD[1]

[1] Hotel-Dieu de France University Medical Center, Department of Pediatric Cardiology, Saint Joseph University, Naccache Boulevard, Achrafieh, Lebanon

[2] Hotel-Dieu de France University Medical Center, Department of Pediatrics, Saint Joseph University, Naccache Boulevard, Achrafieh, Lebanon

Abstract

Objective: **To describe our experience in percutaneous patent ductus arteriosus (PDA) closure using the Occlutech Duct Occluder (ODO).**

Methods: **We retrospectively reviewed records of patients who underwent a PDA closure attempt using the ODO between August 2013 and October 2015. Only patients with isolated PDA and weighing ≥6 kg were eligible for ODO use.**

Results: **Eighteen ODO devices were successfully implanted in 18 patients. Patient age and weight ranged from 6 to 180 months (median, 23.5 months) and 6 to 54 kg (median, 11 kg), respectively. PDAs were of type A (n = 16), type E (n = 1), or type D (n = 1). PDA diameter ranged from 2 to 5 mm (median, 3 mm). Median procedure time was 55 min (range, 35–105 min). Median fluoroscopy time was 9.2 min (range, 3.0–29.6 min). The device diameter (pulmonary end) was 5–8 mm (median, 7 mm). The standard shank length was used in 13 cases, and the long variant was used in five cases. Median follow-up period was 12 months. All devices were successfully implanted. Total occlusion was achieved the following day in all but two patients, in whom it was confirmed one month later. No major complications occurred. Mild pulmonary obstruction was noted in one patient, and aortic disc bulging occurred in two patients without hemodynamic consequences.**

Conclusion: **In this group of patients, the ODO showed excellent results in terms of safety and efficacy. The long device variant may be advantageous in some large and long PDAs. Larger case series are needed to compare the ODO with preexisting devices.**

Key Words

Congenital heart disease • Patent ductus arteriosus • Percutaneous closure • Occlutech

Introduction

Since the first successful transcatheter closure of patent ductus arteriosus (PDA) by Porstmann in 1967 [1, 2], several different PDA closure devices have been developed and evaluated. Today, percutaneous closure of almost any PDA beyond neonatal age can be easily and safely performed using detachable coils or specifically designed occluders, including different generations of the Amplatzer Duct Occluder (ADO I, II, and AS) [3-5]. Nevertheless, some large and long (i.e., "slow tapering") type A PDAs and nonconical large PDAs still pose technical difficulties to the interventionist, especially in small infants.

A new device, the Occlutech Duct Occluder (ODO), has been designed with the aim of addressing some of these challenges. Like the ADO I, the ODO is constructed from braided Nitinol wires, has an aortic

Fax +1 203 785 3346
E-Mail: jshd@scienceinternational.org
http://structuralheartdisease.org/

ISSN 2326-4004

Accessible online at:
http://structuralheartdisease.org/

* Corresponding Author:
Ramy Charbel, MD
Department of Pediatrics
Hotel-Dieu de France University Medical Center, Saint Joseph University
Naccache Boulevard, Achrafieh, Lebanon
Tel.: +961 3 783 560, Fax: +961 1 615 300 ext. 3233, E-Mail: ramycharbel@hotmail.com

Table 1. Comparative table showing characteristics of available Occlutech Duct Occluder devices (manufacturer data).

Shank Type	Introducing System Size (mm)	Aortic Shank Diameter (mm)	Pulmonic Shank Diameter (mm)	Retention Disc Diameter (mm)	Length (mm)
Standard shank	6	3.5	5	9	4.25
Standard shank	6	4	6	10	5.00
Standard shank	6	5	7	11	6.05
Standard shank	6	6	8	13	6.30
Standard shank	7	8	10	16	7.00
Standard shank	7	10	12	18	12.00
Standard shank	8	12	15	20	14.00
Standard shank	9	14	18	24	16.00
Long shank	6	3.5	5	9	7.00
Long shank	6	4	6	10	7.50
Long shank	6	5	7	11	8.50
Long shank	6	6	8	13	9.00
Long shank	7	8	10	16	10.50

mm = millimeters.

retention disc, and is attached to its delivery cable using a screw cap mechanism. Both devices have comparable designs; however, the ODO has a waist that is wider at its pulmonary end than at its aortic end with the purpose of achieving a more stable implant. Moreover, to facilitate use in longer PDAs, the ODO is available in two different lengths.

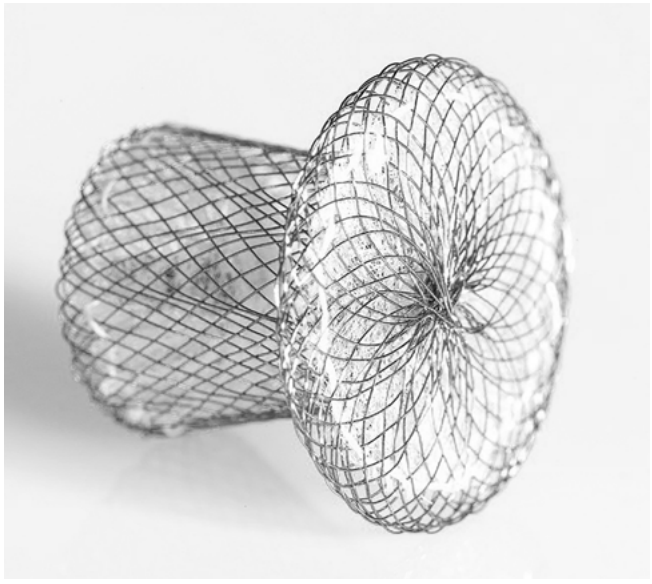

Figure 1. The Occlutech Duct Occluder device (as shown on occlutech.com).

The objective of this study was to investigate the safety, efficacy, and clinical utility of the ODO device.

Materials and Methods

The ODO was introduced to our catheterization unit in August 2013. Since then, our policy has been to prioritize its use over other existing devices in patients with isolated PDA who weigh ≥6 kg to test its safety and efficacy. We retrospectively reviewed records of patients who underwent a PDA closure attempt with the ODO between August 2013 and October 2015.

The Device

The ODO device is made of braided Nitinol threads. Nitinol is a very elastic metal alloy with memory properties. The ODO consists of an aortic disc connected to a cone-shaped shank (Figure 1). Compared with the ADO I device, the direction of the ODO conical body is inverted. The proximal end of the shank (i.e., pulmonic end) has a diameter that is 1.5–2.0 mm larger than that of its aortic end, and the retention disc has a diameter that exceeds the size of the aortic end of the shank by 5.5–8.0 mm. The ODO is available in several sizes, each with a standard (i.e., short) or long shank (Table 1). Polyethylene patches inside the device support immediate closure of the defect. The device is attached to a delivery cable by a screw that, after detachment, protrudes from the pulmonary end of the device to allow easier snaring if retrieval is required. Before January 2015, and because the ODO did not yet have a dedi-

Figure 2. In a 15-year-old female weighing 54 kg, the long variant of the 5-7 Occlutech Duct Occluder was adequately accommodated in a 3-mm type D patent ductus arteriosus.

cated sheath, a Mullins sheath (William Cook Europe, Bjæverskov, Denmark) was used to deploy the device. Since then, a dedicated delivery set including a delivery sheath (6-F to 9-F depending on the implant size), hemostasis valve, dilator, and transparent loader was introduced.

Technique

Informed consent was obtained prior to patient enrollment. All procedures were performed according to the manufacturer's instructions under general anesthesia by the same operator (ZS). In brief, vascular access was obtained via the femoral artery and vein. Heparin (50I U/kg) and Cefazolin (30 mg/kg) were administered intravenously. Lateral aortography was performed to determine the size and shape of the PDA. In some patients, supplementary projections were needed to more accurately delineate the PDA. In PDAs >3 mm, systolic and diastolic diameter variations were carefully measured to determine the maximal diameter of the narrowest PDA segment (i.e., "landing zone") during cardiac cycling. The device size was calculated to fit the diameter of the area where the device was to be "squeezed" into the PDA. For ODO size selection, the aortic end of the device shank was sized to be 1–2 mm larger than the landing zone in smaller PDAs (<3 mm) and 2–3 mm larger in larger PDAs (≥3 mm). The standard ODO variant was used in patients with short PDAs. Use of the long ODO variant was limited to cases in which the operator judged that the pulmonary part of the device would not reach the narrowest part of the duct into the pulmonary artery. Venous delivery was used in all cases.

Before releasing the device, an aortogram to verify device positioning was performed. Additionally, if the device appeared to protrude into the pulmonary artery or the aorta, pulmonary or aortic pullback pressure tracing and angiography were performed to rule out significant obstruction. Repositioning was judged necessary in some cases, but we did not encounter any difficulty in resheathing and redeploying the device in a more suitable manner. After a satisfying position was achieved, the device was released by rotating the delivery cable in a counter-clockwise manner. A final aortogram was performed after the release of the ODO to confirm the position of the device and check for residual shunt or aortic obstruction.

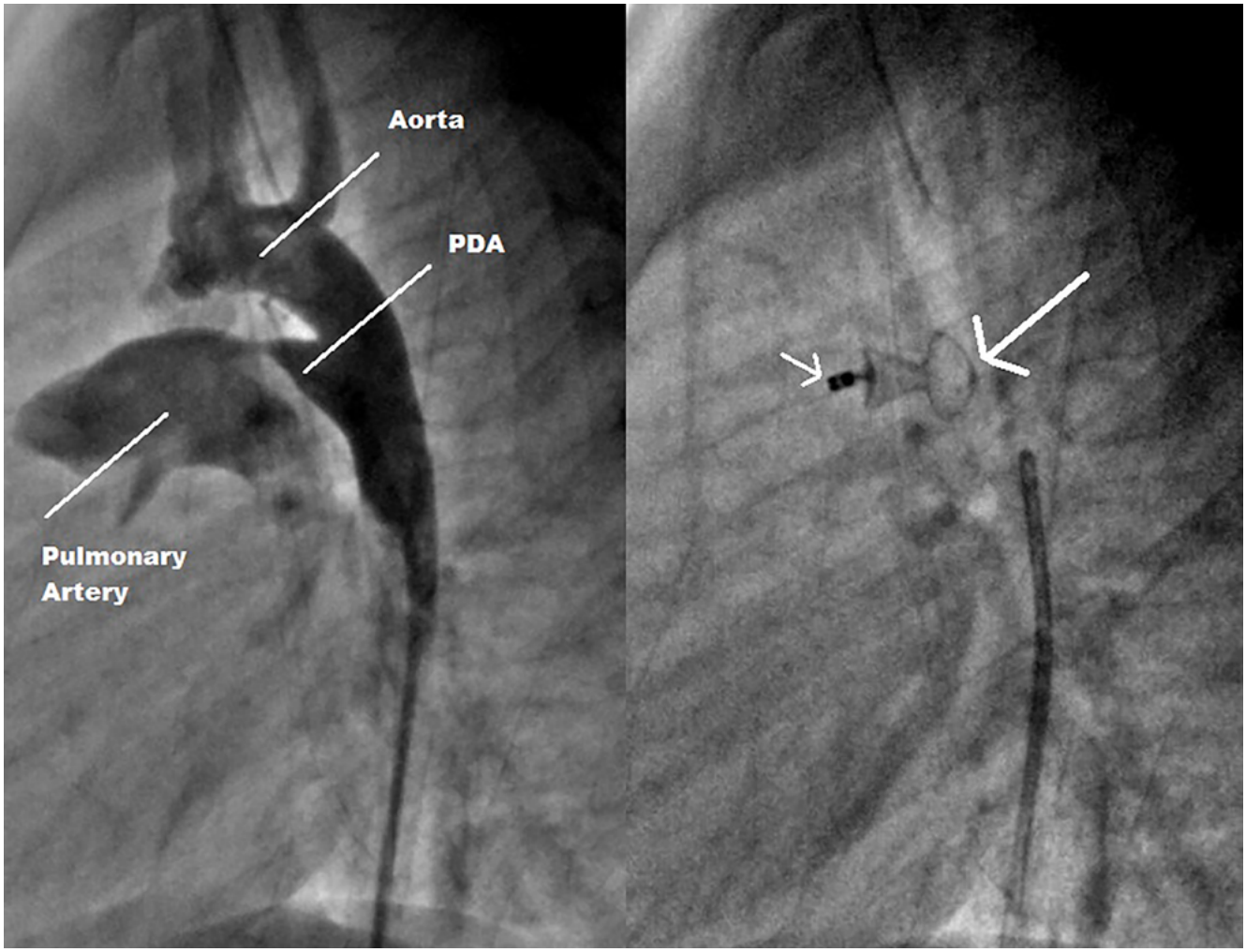

Figure 3. In a 19-month-old boy weighing 10 kg, a 3-mm type A "slow tapering" patent ductus arteriosus was closed using a 5-7 Occlutech Duct Occluder standard shank. The **thick arrow** shows bulging of the aortic disc, probably due to excessive oversizing. Note the screw pin deformation (**thin arrow**), which was related to the forced entry of the device in an incompatible delivery system after multiple attempts due to the lack of a dedicated delivery system at the time.

All 18 patients were discharged 24 hours following the procedure. The following day, chest x-rays (anteroposterior and lateral) and Doppler echocardiography were obtained before discharge. Special attention was paid to residual shunts and left pulmonary or aortic isthmic obstruction. Urinalysis was performed only in cases of residual shunting. Patients were scheduled for cardiology consultation and echocardiography at 10 days and at 1, 3, 6, and 12 months.

Statistical Analysis

Results are expressed as percentages and median values.

Results

The median age of the 18 patients was 23.5 months (range, 6–180 months), and median weight was 11 kg (range, 6–54 kg). All patients had isolated PDAs. Table 2 summarizes the basic characteristics of the patients and procedure-related parameters according to PDA morphology. The PDA shape was type A "fast tapering" in seven patients (40%), type A "slow tapering" in nine patients (50%), type E in one patient, and type D in one patient. The narrowest PDA diameter ranged from 2 to 5 mm (median, 3 mm). Median procedure time was 55 min (range, 35–105 min), and median fluoroscopy time was 9.19 min (range, 3–29.57 min). Device diameters (aortic end) ranged from 3.5 to 6 mm (median, 5 mm); standard device variants were used in 13 patients, and long devices were used in five patients. The median follow-up period was 12

Table 2. Characteristics of patients and procedure-related parameters according to patent ductus arteriosus morphology.

Patient ID	Gender	Age (months)	Weight (kg)	PDA Size (mm)		Fluoroscopy Time (min)	Pulmonic Shank Diameter (mm)	Aortic Shank Diameter (mm)	Shank
Type A fast PDA									
ZS-PDA01	F	48	15.0	2.3	35	3.16	6.0	4.0	Standard
ZS-PDA02	F	6	6.5	5.0	60	10.13	7.0	5.0	Standard
ZS-PDA03	F	7	10.0	3.5	40	3.12	8.0	6.0	Standard
ZS-PDA04	F	72	21.0	2.5	60	14.14	6.0	4.0	Standard
ZS-PDA05	F	12	6.0	2.8	35	5.27	7.0	5.0	Standard
ZS-PDA06	F	13	12.0	3.3	53	6.50	7.0	5.0	Standard
ZS-PDA18	F	60	17.0	5.0	35	3.00	8.0	6.0	Standard
Type A slow PDA									
ZS-PDA07	F	8	9.5	3.0	55	18.70	7.0	5.0	Long
ZS-PDA08	F	27	9.0	3.0	40	13.47	7.0	5.0	Standard
ZS-PDA10	M	19	10.0	3.0	55	3.18	7.0	5.0	Standard
ZS-PDA11	F	84	32.0	2.0	75	29.57	5.0	3.5	Standard
ZS-PDA12	M	24	13.5	3.0	55	9.19	6.0	4.0	Standard
ZS-PDA13	M	23	10.0	3.0	50	9.14	5.0	3.5	Long
ZS-PDA14	M	29	14.0	2.5	65	9.19	6.0	4.0	Long
ZS-PDA15	F	11	7.0	3.8	105	12.33	7.0	5.0	Long
ZS-PDA17	F	48	16.5	2.0	60	10.00	5.0	3.5	Standard
Type D PDA									
ZS-PDA16	F	180	54.0	3.0	55	8.48	7.0	5.0	Long
Type E PDA									
ZS-PDA09	F	15	9.5	3.0	75	11.40	6.0	4.0	Standard

kg = kilograms; mm = millimeters; min = minutes.

months (range, 3–21 months), and all patients were reviewed at 1 month. All 18 devices were successfully implanted. All patients were discharged 24 hours following the procedure, and complete PDA occlusion on Doppler echocardiography was achieved in all but two patients (closure rate, 90%). At 1-month follow-up, all patients had total duct occlusion on Doppler echocardiography (closure rate, 100%).

Successful device placement rate was 100%. There were no mortalities or major complications. Aortic disc bulging occurred in two patients without hemodynamic gradient. Mild pulmonary obstruction was noted in one patient in whom the long device variant was used. A cardiac ultrasound at 6-month follow-up did not show evidence of hemodynamic gradient. No blood transfusions were needed. No hemolysis occurred. There were no femoral vascular complications.

Discussion

PDA Treatment

PDA is a common congenital heart defect usually identified in early childhood. In some cases, it remains unrecognized until late in life. Currently, percutaneous closure of almost any PDA beyond neonatal age using detachable coils or specifically designed oc-

cluders such as the ADO is the "gold standard" [3]. Despite the effectiveness of currently available devices, procedural challenges remain, especially when small infants and/or large PDAs are involved. Moreover, increasing experience with transcatheter techniques has resulted in interventional cardiologists attempting to more frequently treat patients who have PDAs with complex morphologies [6]. Therefore, there still is a demand for an ideal PDA closure device. Theoretically, such a device would have a design adaptable to any shape or size of PDA, regardless of patient age and weight, and achieve immediate closure in 100% of cases. The implantation technique would also be operator-friendly. In addition to addressing current shortcomings, such a device would reduce the need for catheterization laboratories to stock several types of products with different sizes. These remaining unfulfilled needs justify ongoing research and development of new device models.

The ODO Device

The ODO device was developed with the aim of addressing some of the above-mentioned drawbacks. Even though our study was not comparative, the ODO device resembles the ADO I device with respect to design, intended use, and specific application, which provides an "experimental-feeling" comparison between the two devices. In fact, the ODO device material and delivery system and techniques are very similar to those of the ADO I. Notwithstanding these similarities, radical modifications in the shape of the ODO were introduced. The core of the device is wider at the pulmonary end than at the aortic end, the distal clamp at the aortic end (in the ADO) is not present, and the screw attachment protrudes from the pulmonary end. This shape, which resembles a champagne cork, takes advantage of the benefits of both the ADO I (i.e., inflexible connection between the aortic disc and device core) and the ADO II (i.e., aortic and pulmonary retention discs). In addition, retrieval of the device in case of accidental embolization is theoretically easier because the screw protrudes from the pulmonary end after release, making it more accessible for snaring.

Given that the ODO is available in larger sizes than the ADO devices, it allows closure of larger-sized PDAs. In fact, prior to the launch of the ODO, in some studies, patients with large PDAs had to be excluded due to non-availability of larger devices [7]. Another crucial difference from the ADO I is that the ODO comes in two length options: standard and long shank. The long variant may be needed in some "slow tapering" type A or nonconical long and large PDAs. In one patient in our series with a large (3 mm) and long (11 mm) type D PDA, the ODO 5-7 long device was clearly the most suitable (Figure 2). Before the introduction of the ODO, our best option would have been to deploy an ADO I, including its aortic retention disc, in the PDA body. This was in fact successfully performed in a similar case in a previous study [3].

Device Selection

In the first few cases, the size of the aortic end of the occluder shank was chosen based on the narrowest diameter of the PDA, extrapolating our experience with the ADO I. After facing occurrences of aortic disc bulging (Figure 3), probably due to excessive oversizing, we concluded that the shank size should be calculated based on the part to be "squeezed" by the duct. It is worth mentioning that the choice of sizing should take into consideration the systolo-diastolic variations of the duct size, particularly in larger ducts (>3 mm) [8].

Safety and Efficacy

Reported case series in the literature confirm the high occlusive properties of the ODO, even though larger ducts usually require more time to close [8, 9]. Our present results demonstrate a 100% success rate (shunt closure and successful implantation) with zero mortality and no serious morbidity. In fact, we noted a 90% closure rate at day 1, reaching 100% at 1-month follow-up. In our series as well as a recently reported case series of PDA closure with the ODO device, no major adverse events (e.g., accidental device embolization, significant aortic or pulmonary obstruction, endocarditis, hemolysis or vascular injury) were encountered [10]. Considering the high degree of similarity between the Occlutech and Amplatzer devices and that most complications are seen during or shortly after implantation, it is reasonable to infer comparable safety of the two devices. Furthermore, reported late adverse events were very rare [11, 12], and therefore no further major adverse events are expected from studies of the ODO device.

Due to the lack of a dedicated delivery system early in our study, some difficulties were noted while handling the device. We encountered the same drawbacks described by Kudumula et al. [8] and Rioz-Mendez [13] in term of loading and later detaching the device. Nevertheless, these difficulties had minimal impact on our procedure and fluoroscopy times due to the experience of the operator and his familiarity with the ADO, which led to bypassing a substantial amount of the learning curve [12]. Ten cases after the launch of our series, the manufacturers introduced important changes, providing a specific delivery system and thus minimizing further technical problems.

Although aortic embolization of the ADO I was rarely reported, as even relatively long ducts tend to shorten after being pulled back with the device, we found that some longer PDAs would not be appropriately closed with an ADO I and thus required the use of the long variant of the ODO to avoid aortic device dislodgment [3]. The case pictured in Figure 2 highlights the advantage of this variant. However, the long variant of the device can be a double-edged sword if the shortening of the duct after pullback is not taken into consideration. In one patient, the inappropriate use of this variant led to the protrusion of the device in the pulmonary artery with mild, insignificant gradient that completely resolved 6 months later.

Although our study is not comparative, and despite the small number of cases, our experience suggests that the ODO is a safe, effective, and operator-friendly device for PDA closure in patients weighing ≥6 kg with mostly type A PDA. The availability of two different length variants makes the ODO a preferable solution for some long and large type D PDAs. Larger case series and longer follow-up, as well as comparative studies, would provide additional support for our findings. It remains to be determined whether the ODO is capable of replacing all preexisting devices in all patients.

Conflict of Interest

The authors have no conflict of interest relevant to this publication.

Comment on this Article or Ask a Question

References

1. Porstmann W, Wierny L, Warnke H, Gerstberger G, Romaniuk PA. Catheter closure of patent ductus arteriosus: Sixty-two cases treated without thoracotomy. Radiol Clin North Am. 1971;9:203-218. PMID: 4938290
2. Porstmann W, Wierny L, Warnke H. Der Verschluss des Ductus Arteriosus in persistent ohne Thorakotomie Thoraxchirurgie. 1967;15:109-203.
3. Saliba Z, El-Rassi I, Helou D, Chehab G, Abdel-Massih T, Daou L, et al. Analyzing the failures of percutaneous closure of the patent ductus arteriosus in patients over 5 kg. J Invasive Cardiol. 2012;24:434-438. PMID: 22954562
4. Baruteau AE, Hascoet S, Baruteau J, Boudjemline Y, Lambert V, Angel CY, et al. Transcatheter closure of patent ductus arteriosus: Past, present and future. Arch of Cardiovasc Dis. 2014;107:122-132. DOI: 10.1016/j.acvd.2014.01.008
5. Rao PS. Percutaneous closure of patent ductus arteriosus–current status. J Invasive Cardiol. 2011;23:517-520. PMID: 22147400
6. Saliba Z, El-Rassi I, Helou D, Abou-Jaoudeh P, Chehab G, Daou L, et al. Development of catheter-based treatment of patent ductus arteriosus: a medium-sized centre experience. Arch Cardiovasc Dis. 2009;102:111-118. DOI: 10.1016/j.acvd.2008.11.001
7. Al-Hamash SM, Wahab HA, Khalid ZH, Nasser IV. Transcatheter closure of patent ductus arteriosus using Ado device: Retrospective study of 149 patients. Heart Views. 2012;13:1-6. DOI: 10.4103/1995-705X.96658
8. Kudumula V, Taliotis D, Duke C. The new occlutech duct occluder: immediate results, procedural challenges, and short-term follow-up. J Invasive Cardiol. 2015;27:250-257. PMID: 25929302
9. Abdelbasit MA, Alwi M, Kandavello G, Che Mood M, Samion H, Hijazi ZM. The new Occlutech PDA occluder: Initial human experience. Catheter Cardiovasc Interv. 2015;86:94-99. DOI: 10.1002/ccd.25878
10. Jang GY, Son CS, Lee JW, Lee Jy, Kim SJ. Complications after transcatheter closure of patent ductus arteriosus. J Korean Med Sci. 2007;22:484-490. DOI: 10.3346/jkms.2007.22.3.484
11. Abadir S, Boudjemline Y, Rey C, Petit J, Sassolas F, Acar P, et al. Significant persistent ductus arteriosus in infants less or equal to 6 kg: Percutaneous closure or surgery? Arch Cardiovasc Dis. 2009;102:533-540. DOI: 10.1016/j.acvd.2009.04.004
12. Saliba Z, El-Rassi I, Abi-Warde MT, Chehab G, Daou L, Khater D, et al. The Amplatzer Duct Occluder II: a new device for percutaneous ductus arteriosus closure. J Interv Cardiol 2009;22:496-502. DOI: 10.1111/j.1540-8183.2009.00504.x
13. Ríoz-Méndez RE. The New Occlutech Duct Occluder. J Invasive Cardiol. 2015;27:E229.

Cite this article as: Hanna N, Charbel R, Chehab G, Gerbaka B, Saliba Z. The Occlutech Duct Occluder for Patent Ductus Arteriosus. Structural Heart Disease. 2017;3(1):1-7. DOI: http://dx.doi.org/10.12945/j.jshd.2017.16.002

JSHD
Journal of Structural Heart Disease

Original Scientific Article

Journal of Structural Heart Disease, February 2017,
Volume 3, Issue 1:8-14
DOI: http://dx.doi.org/10.12945/j.jshd.2017.16.003

Received: April 5, 2016
Accepted: July 5, 2016
Published online: February 2017

Left Atrial Appendage Morphology in Patients with Non-Valvular Atrial Fibrillation

Sonya Joy, MD[1*], Horst Sievert, MD[1,2], Stefan Bertog, MD[1,3], Timothy Betts, MD[4], Neil Wilson, MD[1,5], Saul Myerson, MD[6]

[1] CardioVascular Center, Frankfurt, Germany
[2] Anglia Ruskin University , Cambridge and Chelmsford, UK
[3] Interventional Cardiology Veterans Administration Medical Center, University of Minnesota, Minneapolis, USA
[4] Oxford University Hospitals NHS Trust, Oxford, UK
[5] Childrens Hospital Colorado, Colorado, USA
[6] University of Oxford Centre for Clinical Magnetic Resonance Research, Oxford, UK

Abstract

Aims: **Percutaneous left atrial appendage (LAA) occlusion has now become a suitable alternative to oral anticoagulation for stroke prevention in selected patients with atrial fibrillation (AF). However, LAA closure can be technically challenging and results suboptimal, in part due to variable left atrial anatomy.We aimed to characterize LAA morphology and identify potential anatomical pitfalls during LAA closure or LAA thrombus detection during transoesophageal echocardiography (TOE).**

Methods and Results: **103 patients with AF underwent cardiac magnetic resonance angiography to assess pulmonary venous anatomy. Adequate imaging quality was present in 76 in whom LAA morphology was assessed. The majority of LAAs (71%) were anterolaterally directed and 82% were 'claw'-shaped. However, there was significant variation in anatomy and course in the remainder: 11% were anteverted, 9% laterally directed and 9% retroverted. The shape was cone-like in 8%, fan-like in 5% and s-configured in 5% and there was significant variation in the curvature of the LAA body. While 66% had a single lobe, 30% were bilobed and 4% trilobed; 90% also had additional lobules.**

Conclusion: **Our results demonstrate the significant variability of LAA geometry in AF patients. This may have implications for future device design for percutaneous LAA occlusion. The variable anatomy may affect LAA thrombus detection with TOE emphasizing the importance of multiple views to ensure complete assessment.**

Key Words

Left atrial appendage • Left atrial appendage morphology • Left atrial appendage closure • Atrial fibrillation

Introduction

Stroke is the most devastating atrial fibrillation (AF)-related event. Non-valvular chronic AF is associated with a more than 5-fold increase in stroke risk [1], with the left atrial appendage (LAA) as the site of thrombogenesis in more than 90% of stroke victims [2]. Although oral anticoagulation with warfarin reduces this risk by more than half [3, 4], only 50–70% of patients with AF who are eligible for anticoagulation actually receive it. Novel anticoagulants are at least as effective as warfarin, but a significant bleeding risk remains. Thus, alternative options for stroke prevention are needed, particularly for patients with contraindications to anticoagulation.

Percutaneous LAA closure has the advantage of obviating long-term anticoagulation. The PROTECT-AF trial demonstrated that percutaneous LAA

Fax +1 203 785 3346
E-Mail: jshd@scienceinternational.org
http://structuralheartdisease.org/

ISSN 2326-4004

Accessible online at:
http://structuralheartdisease.org/

* Corresponding Author:
Horst Sievert, MD
Cardiovascular Center
Seckbacher Landstrasse 65, 60389 Frankfurt, Germany
Tel. +49 69 4603-1343, Fax: +49 69 4603-1343, E-Mail: horstsievertmd@aol.com

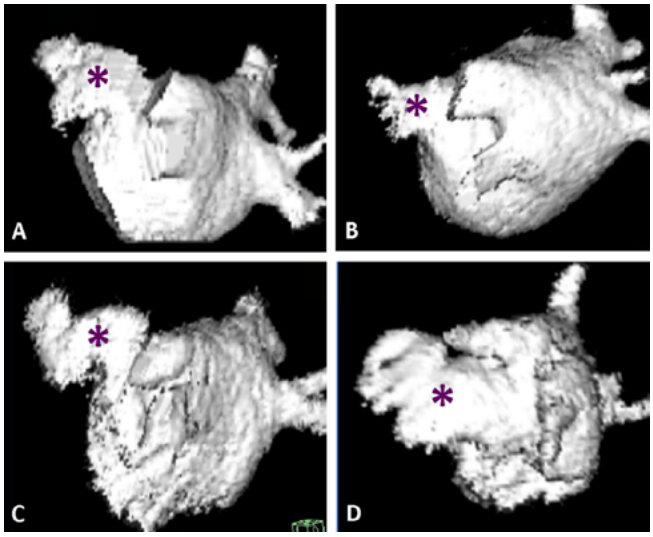

Figure 1. Representative left atrial appendage morphologies (three-dimensional surface rendered angiographic images). *Panel A*. Bi-lobed. *Panel B*. Fan-shaped with three small lobules. *Panel C*. s-configured. *Panel D*. Very large fan-shaped with secondary anterior lobe and multiple lobules. All images are viewed from a similar left postero-lateral position; the left atrial appendage is indicated by an asterisk (*).

closure is at least as safe and effective as anticoagulation with warfarin with regard to all-cause mortality and stroke risk [5]. LAA-occlusion devices have a fixed shape designed to provide an effective seal and stable positioning, but this may not take into account significant variability in LAA shape, orientation, and structure. Furthermore, regardless of the LAA closure device used, co-axial alignment of the delivery sheath within the appendage is crucial for safe and successful implantation, and this depends on the orientation of the LAA. Suboptimal alignment of the delivery system within the appendage may cause perforation [5, 6] and poor final device position, potentially promoting residual leaks [7] and thrombus formation. These complications remain the Achilles heel of the procedure, partially offsetting its potential benefits.

In addition, variation in LAA anatomy may influence the detection of LAA thrombus during transoesophageal echocardiography (TOE). Thrombus located in accessory or retroverted lobes might escape recognition in the usual TOE views, which may partially explain the small incidence of stroke despite TOE interrogation of the LAA prior to cardioversion [8]. Hence, a good understanding of LAA anatomy and orientation is important. Several studies have highlighted variations in LAA anatomy, particularly focusing on LAA size, branches/lobes, or orifice diameter [9, 10]. Few studies, however, have described LAA orientation and shape, which are important for device and delivery system design [11, 12].

Here, we examined the range of three-dimensional (3-D) anatomy and 2-D geometry of the LAA in patients with non-valvular AF to allow sheath configuration and device design improvements that facilitate delivery and deployment. In addition, recognition of unusual anatomical variants may prompt clinicians to interrogate the LAA in all dimensions, which could improve thrombus detection.

Materials and Methods

Study Population

The population consisted of 103 consecutive patients with non-valvular AF who underwent left atrial and pulmonary vein (PV) angiograms using cardiovascular magnetic resonance (CMR) for the purpose of PV isolation ablation (94%), evaluation for possible PV stenosis after PV isolation ablation (5%), or cardiac surgery (1%). The 3-D datasets were processed to ensure good visualization of the LAA and PVs. Twenty-seven patients were excluded due to inadequate image quality. In the remaining 76 patients in whom the LAA was analyzed, 67% were male and 33% were female, with a mean age of 56 ± 11 years (range, 18–77 years).

CMR Scanning and Image Processing

Scans were performed using a 1.5-Tesla magnetic resonance scanner (Siemens Avanto, Siemens Medical Imaging, Erlangen, Germany) at the University of Oxford Centre for Clinical Magnetic Resonance Research. After obtaining localizer images, 3-D contrast-enhanced MR angiograms were acquired using a spoiled gradient echo sequence in a coronal voxel positioned to include the whole left atrium and proximal PVs and timed to the first passage of gadolinium contrast in the left atrium following a test bolus of 2 mL gadolinium contrast. The sequence was acquired during a single 20–30-s breath-hold and was not ECG-gated; scan parameters: TE, 1.1 ms; TR, 3.0 ms; flip angle, 25°; FoV, 360–400 mm; slice thickness, 1.2 mm; 96 slices per slab (slab thickness, 115 mm); and iPAT factor, 3 (GRAPPA). Contrast enhancement was achieved with 0.15 mmol/kg body weight of gadodiamide (Omniscan®, GE Healthcare, Cleveland, OH, USA) administered via an ante-cubital vein at 6 mL/s followed by a saline flush of 20 mL at the same injection rate. After acquisition, data were processed using Siemens Argus software to generate a 3-D surface-rendered image of the left atrium including the LAA. Surrounding structures, such as the aorta, right ventricle, and any residual pulmonary arteries were carefully edited out of the image. This 3-D model was used for assessment of LAA shape, orien-

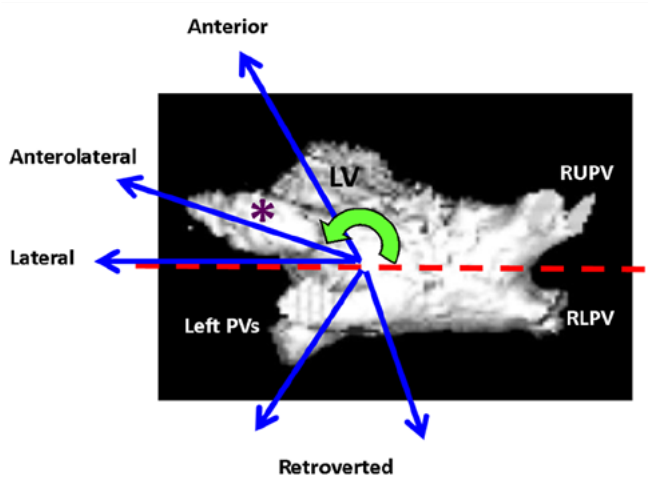

Figure 2. Three-dimensional surface-rendered image of the left atrium viewed from above (superior view) demonstrating the potential major directions of the left atrial appendage (LAA; blue arrows) relative to a coronal plane through the center of the left atrium (red dashed line). The LAA in this figure, marked by an asterisk (*), is in an anterolateral orientation. The green arrow indicates the angle of orientation measured from the coronal plane with zero in the right lateral position. LV, left ventricle; PVs, pulmonary veins; RUPV, right upper pulmonary vein; RLPV, right lower pulmonary vein.

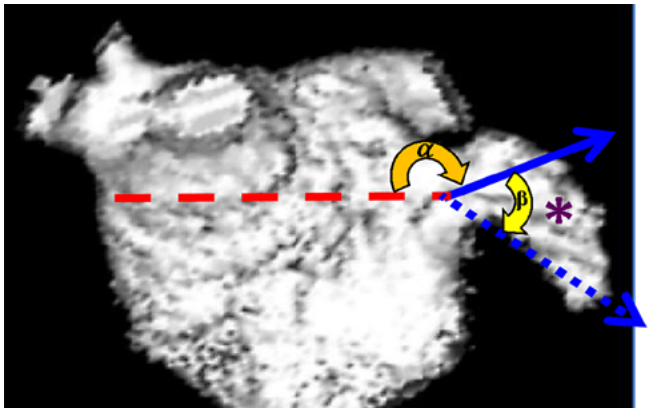

Figure 3. Left atrium viewed from the anterior (ventral) surface demonstrating the angulation of the left atrial appendage (LAA), which is marked by an asterisk (*). The red dashed line indicates the horizontal (i.e., transverse) plane. The solid blue arrow indicates the direction of the proximal tubular portion of the LAA, and the orange blocked arrow indicates the angle between this and the horizontal plane (α). The blue dashed arrow indicates the line from the LAA origin to the tip, and the yellow blocked arrow indicates the change in angle between this and the solid blue arrow (β).

tation, and lobes/lobules, rotating the image when necessary to obtain an optimal view. Further 2-D slices through relevant regions were used to determine other geometrical measures (e.g., angles) as detailed below.

LAA Morphology and Orientation Ascertainment

Shape. LAA shape was categorized into: claw-shaped, fan-shaped, cone-shaped, or s-configured (Figure 1C). Cone-shaped LAAs narrowed to a tip at their distal point without any curvature, whereas claw-shaped LAAs had a single curve, and s-configured LAAs had a double curve. Fan-shaped LAAs were thin and flat, with the maximal width in one direction at least twice that in the perpendicular plane. The morphology of LAAs with complex shapes was categorized based on its closet resemblance to one of the four pre-defined morphologies. We preferred to use standard anatomical/geometric descriptions rather than pictographic descriptions (e.g., chicken wing, cactus) due to inconsistencies in these pictographic shapes.

Orientation/Angulation. The orientation of LAAs was classified according to the major direction of the tip relative to the LAA orifice in an axial plane. This orientation was defined more precisely by determining the angle between a coronal plane through the center of the left atrium and the major longitudinal axis of the LAA when viewed from above. Based on this angle, LAAs were assigned to the following categories: anteverted (≤110°), anterolaterally directed (111 to 150°), laterally directed (151 to 180°), or retroverted (>180°), with the major axis passing dorsally to a coronal section through the LAA orifice (Figure 2). Multi-lobed LAAs (in which lobes often lie in different planes) were classified according to the orientation of the largest lobe. For twisted, multi-directional LAAs, analysis was performed in the direction of the major LAA part.

Precise measurement of LAA curvature is difficult; whereas identification of the long axis of the tubular neck is relatively easy, identification of the distal long axis is hindered by unclear tubular lines. We therefore examined the angulation of the proximal LAA neck (assessed as the angle between a transverse plane through the LAA orifice and the major longitudinal axis of the proximal LAA (angle α, Figure 3) in addition to measuring the change in angle between this line through the proximal LAA and a line from the orifice to the tip (angle β, Figure 3). These provide an indication of the degree of proximal angulation and curvature of the rest of the LAA. In multi-lobed LAAs, analysis was performed on the major lobe. The change in angle was categorized as stable (0°), mild increase (1 to 30°), moderate increase (31 to 60°), or severe increase (>60°), with corresponding categories for negative values (superior/retroverted angulation).

Number of Lobes and Lobules. LAAs were considered to have at least one lobe (i.e., a tubular body with a blind-ending sac). If at least one cleft split the LAA by at least 50% of its length, the regions on either side of the cleft(s) were deemed to be separate lobes (Figure 1A). Further criteria, we took into consideration, were the ones defined by Veinot et al. [9]: a visible outpouching from the main tubular body of the LAA (usually demarcated by an external crease) that was (1) occasionally but not necessarily associated with a change in direction

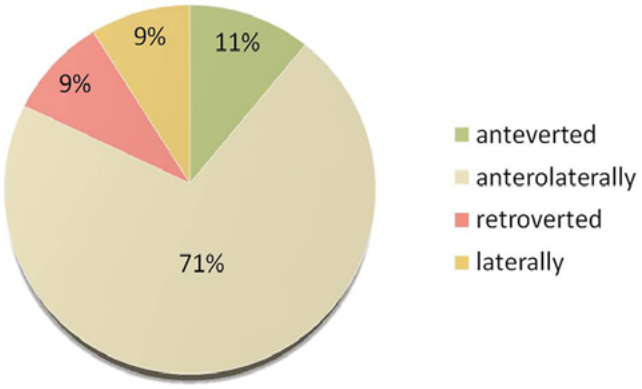

Figure 4. Distribution of different left atrial appendage (LAA) positions/orientations. Anteverted (≤110°), anterolaterally directed (111 to 150°), laterally directed (151 to 180°), or retroverted (>180°, with the major axis passing dorsally to a coronal section through the LAA orifice).

of the main tubular body of the LAA or (2) lying in a different anatomic plane to the main tubular body. Lobules were defined by a clear separate pouch from the main lobe but with a division/cleft of the lobe by less than 50% (Figure 1B and 1D).

Statistical Analysis

Categorical data are reported as percentages, and group comparisons were performed using Fisher's exact tests. Group comparisons for continuous data were performed using Wilcoxon-Mann-Whitney U tests. Normally distributed continuous variables (according to David's test) are expressed as mean ± standard deviation (SD). In histograms, the number of class divisions was calculated by the root of the sample size. *P*-values < 0.05 were considered to indicate statistical significance. Statistical analyses were performed using BiAS. for Windows 9.10 Software (Johann Wolfgang Goethe-University, Frankfurt, Germany).

Results

Shape

Most LAAs were claw-shaped (82%), including all retroverted LAAs. The remaining LAAs were fan-shaped (5%), cone-shaped (8%), or s-configured (5%).

Orientation/Angulation

Most LAAs were anterolaterally directed when viewed from above (78%), although a sizeable minority of LAAs were retroverted (9%), with the remainder being anteriorly or laterally directed (Figure 4). The ranges and frequencies of orientation were similar between sexes, with a slightly higher frequency of retroverted LAAs in women (16%) than in men (6%), although the sample sizes were small. The angulation of the proximal LAA (angle α) ranged widely, from 77 to 160° (mean, 125 ± 16°). In 75% of individuals, angle α was between 110 and 140°, including the majority of retroverted LAAs (6 out of 7; Figure 5A). Almost two-thirds of LAAs (58%) had a mild or moderate increase in curvature (angle β, 1 to 60°) between the proximal and most distal part of the LAA (Figure 5B). Most retroverted LAAs had a significant change in angle (-30 to -90°). A minority of claw-shaped LAAs had no change in angle (8%). Likewise, all cone-shaped LAAs, by virtue of their definition, had no change in angle.

Lobes and Lobules

Of all appendages, 66% had a single lobe, 30% were bi-lobed, and 4% were tri-lobed. The mean number of lobes was 1.4 ± 0.6, with a range from 1 to 3. Six of the seven retroverted LAAs consisted of one lobe, with the remaining one having two lobes. The majority of patients had at least one additional lobule (90%), with a mean number of 2.0 ± 1.2 lobules (range, 0–5), which tended to be located at the tip of a lobe.

Discussion

While most patients had a classical (i.e., claw-shaped) LAA shape and curvature, we found significant variation in LAA orientation, shape, and curvature, with unusual shapes in 18% of patients, retroverted LAAs in approximately 10% of patients, and a wide range of angulations and multiple lobes in 90% of patients. This may have significant implications for clinical practice during LAA closure or the identification of LAA thrombus by TOE.

TOE-Guided Thrombus Detection

Despite the utility of TOE for thrombus detection in the LAA [13], a small number of thromboembolic events continue to occur even when no thrombus is detected in a pre-cardioversion [8] or LAA-occlusion setting (1–2%) [5, 6]. Possible causes include absent or sub-therapeutic anticoagulation [14] and air embolism due to insufficient venting during LAA occlusion [5]. It is conceivable that thrombi may be missed during TOE examination, particularly in patients with retroverted LAAs and/or multiple lobes and large an-

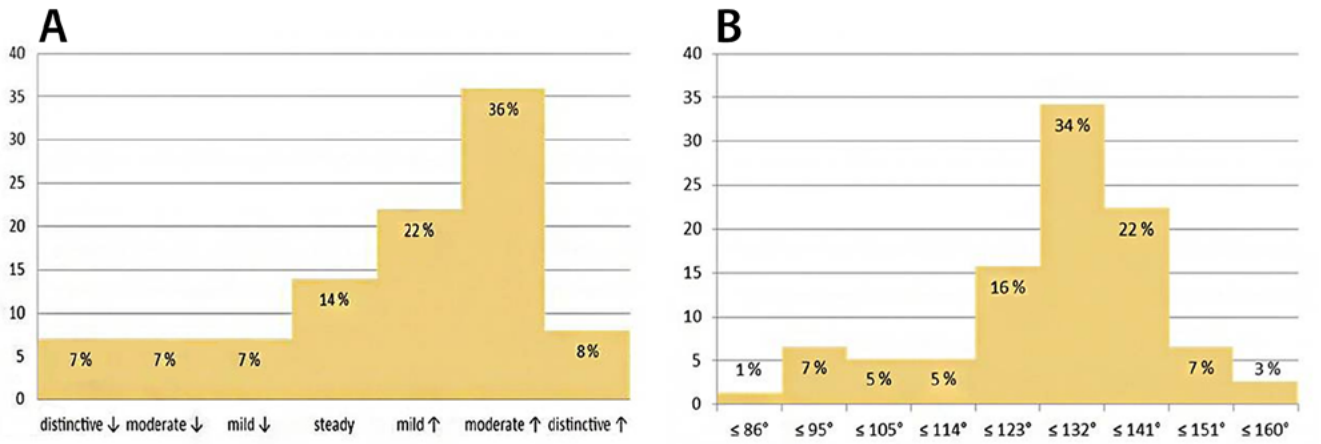

Figure 5. *Panel A and Panel B.* Distribution of *(Panel A)* the angulation of the proximal tubular portion of the left atrial appendage (LAA) to the horizontal plane (angle α, see Figure 3) and *(Panel B)* the change in LAA curvature (angle β, see Figure 3).

gulations, in whom complete imaging would require LAA interrogation in multiple views.

Although most LAAs in our study (77%) were anterolaterally directed, retroverted LAAs were found in 9% of patients. Previous studies using computed tomography (CT) angiography, invasive angiography, and cadaveric materials have reported the presence, but not the frequency, of retroverted LAAs [15, 16]. Some retroverted LAAs can appear relatively normal on standard views (typically mid-esophageal, with a beam angulation of 75°), with an apparent apex at the angulated bend. As a result, ensuring the identification of any retroverted lobes requires comprehensive assessment with multiple angulations of the ultrasound beam, which are not routinely employed. Our study highlights the variable LAA morphology that can complicate TOE-guided thrombus detection and emphasizes the importance of LAA imaging in all planes and angles, keeping in mind that retroverted appendages and/or multiple lobes are common. Although our findings suggest a slightly higher prevalence of retroverted LAAs among females than males, the small sample sizes limit our ability to draw firm conclusions. Further studies on this subject might be important due to the higher risk of AF-related stroke in women in the presence of other risk factors (e.g., CHA_2DS_2-VASc score) [17].

Interventional LAA Closure

The significant variation in shape, orientation, and curvature of the LAA is important for LAA closure device design and procedural technique. As the thin walls of the LAA (muscular wall ≤1 mm) are vulnerable, device maneuvering during the procedure [18] together with anatomical variation in the LAA may partly explain the most common (4–5%) [5, 6] risk of perforation and pericardial hemorrhage. Malalignment of the delivery system with the central axis of the LAA may cause tension/stress on the LAA or may result in suboptimal device positioning, leading to more manipulations including device recapturing and redeployment.

Although no trials exist to confirm this, many operators would agree that greater manipulation during delivery system alignment and device positioning carries a higher risk of perforation and hemorrhage. Entering the LAA and subsequent occluder release require alignment along the axis of the LAA body/proximal LAA. This angle (α) was between 110° and 140° in 75% of LAAs in our study, including the majority of retroverted LAAs (6 out of 7). With the current WATCHMAN LAA occlusion device, the delivery sheath must be inserted to a depth equal to at least that of the maximum ostial diameter (21–33 mm). In acutely angled appendages, particularly those that are retroverted, this may add to the complexity of the procedure. Similarly, the Amplatzer Cardiac Plug requires a proximal landing zone of at least 10 mm to deploy the distal lobe of the device. Thus, the curvature of the LAA is also important, and in 58% of cases, we observed a mild to moderate increase in angle (1 to 60°). This change in angle was greater in retrovert-

ed LAAs, with one half showing a moderate decrease and the other showing a severe decrease in angle (-30 to -90°). This combination of unusual direction and change in curvature may complicate deep insertion of the WATCHMAN device into the LAA. Our characterization of LAA morphology could improve delivery system design to facilitate access to the LAA and may provide guidance for catheter tip configuration, allowing smoother positioning within the LAA. These improvements have the potential to reduce the risk of perforation and pericardial hemorrhage. Optimally, multiple delivery sheaths with a variety of curvatures that approximate angulations of the appendage assessed with non-invasive imaging such as CT or MRI together with pre-procedural characterization of the LAA with respect to its angulation and curvature would minimize the need for undue sheath manipulation and device recapture maneuvers.

LAA Lobes and Lobules

Complete LAA assessment and closure is complicated by multi-lobed appendages, as lobes can exist in different planes requiring complex visualization in multiple views. Our results regarding the number of lobes are consistent with those of Heist et al. [10], who also used MRI to analyze the LAA in AF patients and found that about two-thirds of LAAs had one lobe, one-third had two lobes, and a small proportion (<5%) had multiple lobes (≥3 lobes). However, Veinot et al. [9] found a much higher prevalence of multiple lobes in post-mortem specimens of normal hearts, with 80% of LAAs having more than one lobe. These discrepancies among studies may arise from differences in lobe definitions and a lack of distinction between lobes and smaller variants (i.e., lobules). In addition, further extra- and intraluminal criteria (i.e., an external crease and accessibility by a probe, respectively) potentially increasing the number of lobes were taken into account by Veinot et al. but could not be assessed in our study due to different analytical methods. Finally, identification of small lobules may have been more difficult in our study due to smaller spatial resolution by non-gated MRI compared with direct visualization in post-mortem studies.

Limitations of our study include a small sample size; therefore, quoted proportions should be regarded as approximate. However, our study was undertaken to demonstrate the range of shapes and angulations that can occur in LAAs to avoid the assumption of uniform geometry rather than to report precise proportions of each morphology. Twenty-seven patients with inadequate image quality for LAA assessment were excluded, which in theory may have led to selection bias. However, such a bias would have required that LAA morphology affected CMR image quality, which is unlikely as this is not dependent on LAA orientation. Most importantly, we performed our analysis based on the assumption that knowledge of LAA morphology and recognition of its variants may lead to improvements in device and delivery system designs, thereby reducing the risk of procedural complications. Though plausible to operators, this assumption remains to be proven. Our study population consisted only of patients with current/paroxysmal AF, who may likely have larger left atria. Although this could alter LAA shape, significant modifications seem unlikely. Furthermore, these patients are also those in whom TOE assessment for thrombus or LAA device closure is usually performed; therefore, they are a valid group to study.

Our finding that the morphology and orientation of the LAA can vary significantly may have implications for clinical practice. Retroverted LAAs and multiple LAA lobes are common, and the shape and curvature/angulation displays wide variation. Knowledge of these morphological aspects may improve the detection of LAA thrombus on TOE and may also improve delivery sheath configuration and LAA occlusion device design to reduce procedural risk.

Acknowledgements

Saul G Myerson is funded by the Oxford National Institute for Health Research (NIHR) Biomedical Research Centre Program.

Conflict of Interest

The authors have no conflict of interest relevant to this publication.

References

1. Wolf PA, Dawber TR, Thomas HE Jr, Kannel WB. Epidemiologic assessment of chronic atrial fibrillation and risk of stroke: the Framingham study. Neurology 1978;28:973-977. DOI: 10.1212/WNL.28.10.973
2. Blackshear JL, Odell JA. Appendage obliteration to reduce stroke in cardiac surgical patients with atrial fibrillation. Ann Thorac Surg 1996;61:755-759. DOI: 10.1016/0003-4975(95)00887-X
3. Hart RG, Benavente O, McBride R, Pearce LA. Antithrombotic therapy to prevent stroke in patients with atrial fibrillation: A meta-analysis. Ann Intern Med 1999;131:492–501. DOI: 10.7326/0003-4819-131-7-199910050-00003
4. Camm AJ, Lip GY, De Caterina R, Savelieva I, Atar D, Hohnloser SH, et al. ESC Committee for Practice Guidelines (CPG). 2012 focused update of the ESC Guidelines for the management of atrial fibrillation: an update of the 2010 ESCGuidelines for the management of atrial fibrillation. Developed with the special contribution of the European Heart Rhythm Association. Eur Heart J2012;33:2719-2747. DOI: 10.1093/eurheartj/ehs253
5. Reddy VY, Sievert H, Halperin J, Doshi SK, Buchbinder M, Neuzil P, et al. PROTECT AF Steering Committee and Investigators. Percutaneous left atrial appendage closure vs warfarin for atrial fibrillation: a randomized clinical trial. JAMA 2014;312:1988-1998. DOI: 10.1001/jama.2014.15192
6. Park JW, Bethencourt A, Sievert H, Santoro G, Meier B, Walsh K, Lopez-Minquez JR, et al. Left atrial appendage closure with Amplatzer cardiac plug in atrial fibrillation: initial European experience. Catheter Cardiovasc Interv 2011;77:700-706. DOI: 10.1002/ccd.22764
7. Viles-Gonzalez JF, Kar S, Douglas P, Dukkipati S, Feldman T, Horton R, et al. The clinical impact of incomplete left atrial appendage closure with the Watchman Device in patients with atrial fibrillation: a PROTECT AF (Percutaneous Closureof the Left Atrial Appendage Versus Warfarin Therapy for Prevention of Stroke in Patients With Atrial Fibrillation) substudy. J Am Coll Cardiol 2012;59:923-929. DOI: 10.1016/j.jacc.2011.11.028
8. Black IW, Fatkin D, Sagar KB, Khandheria BK, Leung DY, Galloway JM, et al. Exclusion of atrial thrombus by transesophageal echocardiography does not preclude embolism after cardioversion of atrial fibrillation. A multicenter study. Circulation 1994;89:2509-2513. DOI: 10.1161/01.CIR.89.6.2509
9. Veinot JP, Harrity PJ, Gentile F, Khandheria BK, Bailey KR, Eickholt JT, et al. Anatomy of the normal left atrial appendage: a quantitative study of age-related changes in 500 autopsy hearts: implications for echocardiographic examination. Circulation 1997;96:3112-3115. DOI: 10.1161/01.CIR.96.9.3112
10. Heist EK, Refaat M, Danik SB, Holmvang G, Ruskin JN, Mansour M. Analysis of the left atrial appendage by magnetic resonance angiography in patients with atrial fibrillation. Heart Rhythm 2006;3:1313-1318. DOI: 10.1016/j.hrthm.2006.07.022
11. Di Biase L, Santangeli P, Anselmino M, Mohanty P, Salvetti I, Gili S, et al. Does the left atrial appendage morphology correlate with the risk of stroke in patients with atrial fibrillation? Results from a multicenter study. J Am Coll Cardiol 2012;60:531-538. DOI: 10.1016/j.jacc.2012.04.032
12. Lacomis JM, Goitein O, Deible C, Moran PL, Mamone G, Madan S, et al. Dynamic multidimensional imaging of the human left atrial appendage. Europace 2007;9:1134-1140. DOI: 10.1093/europace/eum227
13. Wheeler R, Masani ND. The role of echocardiography in the management of atrial fibrillation. Eur J Echocardiogr 2011;12:133-138. DOI: 10.1093/ejechocard/jer124
14. Khan IA. Transient atrial mechanical dysfunction (stunning) after cardioversion of atrial fibrillation and flutter. Am Heart J 2002;144:11-22. DOI: 10.1067/mhj.2002.123113
15. Sievert H, Qureshi SA, Wilson N, Hijazi ZM. Percutaneous Interventions for Congenital Heart Disease. Informa Healthcare 2007;1st edition:582. DOI: 10.3109/9780203018262
16. Ho SY, McCarthy KP. Anatomy of the left atrium for interventional electrophysiologists. Pacing Clin Electrophysiol 2010;33:620-627. DOI: 10.1111/j.1540-8159.2009.02659.x
17. Lip GY, Nieuwlaat R, Pisters R, Lane DA, Crijns HJ. Refiningclinical risk stratification for predicting stroke and thromboembolismin atrial fibrillation using a novel risk factor-based approach: The euro heart survey on atrial fibrillation. Chest 2010;137:263–272. DOI: 10.1378/chest.09-1584
18. Su P, McCarthy KP, Ho SY. Occluding the left atrial appendage: anatomical considerations. Heart 2008;94:1166-1170. DOI: 10.1136/hrt.2006.111989

Cite this article as: Joy S, Sievert H, Bertog S, Betts T, Wilson N, Myerson S. Left Atrial Appendage Morphology in Patients with Non-Valvular Atrial Fibrillation. Structural Heart Disease. 2017;3(1):8-14. DOI: http://dx.doi.org/10.12945/j.jshd.2017.16.003

JSHD
Journal of Structural Heart Disease

Original Scientific Article

Journal of Structural Heart Disease, February 2017,
Volume 3, Issue 1:15-27
DOI: http://dx.doi.org/10.12945/j.jshd.2017.16.005

Received: April 18, 2016
Accepted: June 10, 2016
Published online: February 2017

Challenges in Atrial Septal Defect Occlusion

Roie Tal, MD[1], Moshe Dotan, MD[2], Yitzhack Schwartz, MD[1], Avraham Lorber, MD[1*]

[1] Pediatric Cardiology and Adults with Congenital Heart Disease Institute, Rappaport Children's Hospital, Rambam Health Care Campus, Haifa, Israel

[2] Pediatric Cardiology, Ziv Medical Center, Safed, Israel

Abstract

We present 11 cases of percutaneous transcatheter occlusion of atrial septal defects (ASDs) in adults, including multi-fenestrated ASD, balloon-assisted deployment of ASD occlude, dilator-assisted deployment of ASD occlude, "cobra"-shaped disfiguration of the left disc, ASD with deficient aortic rim, pulmonary vein-assisted deployment of ASD occlude, "high" ASD, large Chiari network, double interatrial septum, snaring a runaway occluder, and right ventricular diastolic dysfunction causing cyanosis. Each case is followed by a practical discussion of the special dilemmas, complications, and challenges that may occur during common procedures.

Key Words

Atrial septal defect • Percutaneous occlusion • Challenge • Technique

Introduction

Atrial septal defects (ASDs) account for 10–17% of congenital cardiac anomalies. Percutaneous closure of ostium secundum ASD is a safe and effective alternative to surgery [1]. Nevertheless, as with any interventional procedure, some ASD closures pose challenges and dilemmas to the interventional cardiologist. We report a variety of 11 representative cases, highlighting challenging morphological and clinical considerations that are of educational and practical value and suggesting ways to avoid pitfalls and complications. These observations were collected over an 18-year period during which we have implanted over 1,000 interatrial shunts using the percutaneous approach.

Multi-Fenestrated ASD

A 45-year-old patient was evaluated after a cerebrovascular attack. Transthoracic echocardiography (TTE) revealed a floppy interatrial septum (IAS) with four fenestrations (Figure 1). A spontaneous left-to-right flow was noted as well as free right-to-left micro-bubble flow during the Valsalva maneuver. We decided to close the fenestrations with a single device. A first attempt with a 15-mm device deployed in

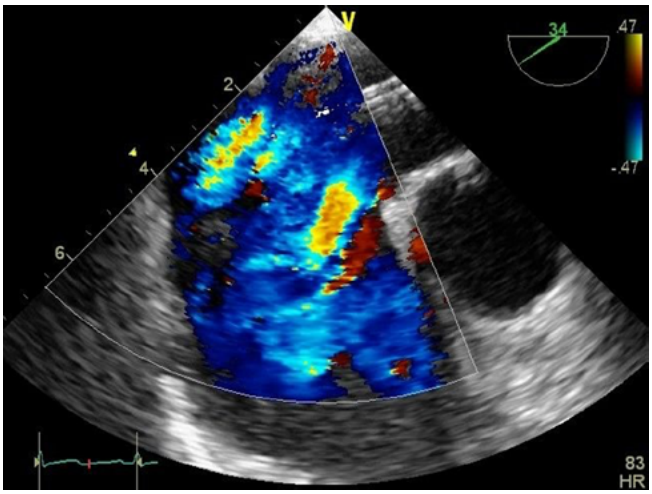

Figure 1. Transesophageal echocardiogram demonstrating a multifenestrated atrial septal defect with four openings.

Fax +1 203 785 3346
E-Mail: jshd@scienceinternational.org
http://structuralheartdisease.org/

ISSN 2326-4004

Accessible online at:
http://structuralheartdisease.org/

* Corresponding Author:
Avraham Lorber
Pediatric Cardiology and Adults with Congenital Heart Disease Institute
Rappaport Children's Hospital, Rambam Health Care Campus
HaAliya HaShniya St 8, Haifa, 3109601, Israel
Tel. +1 972 4 7774630, Fax: +1 972 4 7774690, E-Mail: a_lorber@rambam.health.gov.il

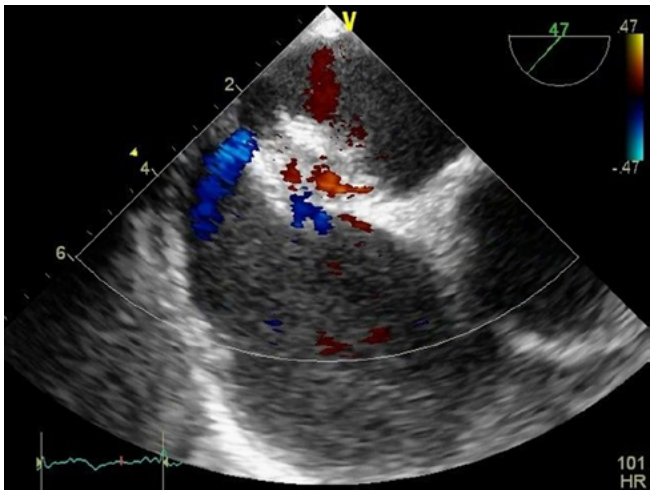

Figure 2. Transesophageal echocardiogram demonstrating a deployed occluding device in one of the atrial septal defects. A leak is present outside the perimeter of the device.

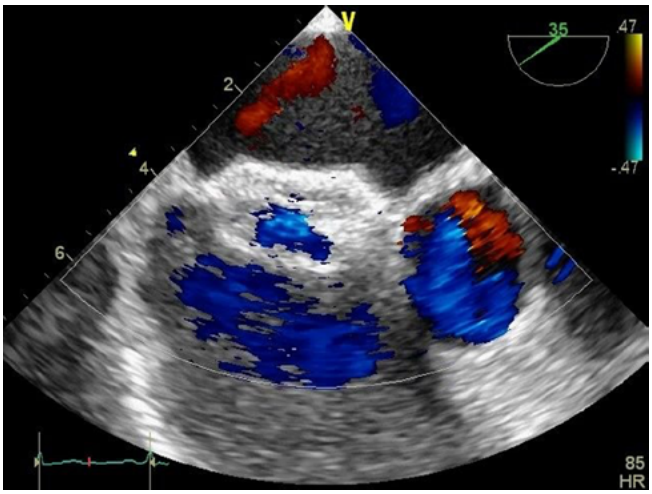

Figure 3. Transesophageal echocardiogram demonstrating a deployed occluding device in one of the atrial septal defects. Residual shunt is present within the perimeter of the device.

one of the central defects failed to occlude all openings (Figure 2). A second attempt was performed in the adjacent central defect using a 21-mm occluder. Residual leak was demonstrated only within the perimeter of the device (Figure 3). At this stage, the device was released.

The transcatheter closure of a multiple or fenestrated ASD can be accomplished by several methods [2]. The defects can be closed by the use of several devices, with each implanted to close one or more defect. When the distance between the ASDs is greater than 7 mm, placement of two devices is recommended [3]. Closure of the larger defect should be performed first [3, 4]. The second device may then need to be larger to overlap the rim of the first device, despite the smaller stretched diameter of the defect. When using more than one device, attention should be paid to maintaining adequate distance from structures like vena cavae entrances and the coronary sinus. The devices might interfere with blood flow and even increase the risk of thrombosis. This, however, has not been apparent in follow-up studies, even after cessation of antiplatelet therapy [5]. In addition, the devices might cause erosion of important tissues, including the aortic root, atrioventricular valves, or atrial free walls. Nevertheless, closure of multiple ASDs using multiple occluders seems to be a safe and effective method. Also, a financial issue that should be considered when implanting more than one device is the reimbursement system used by current health maintenance organizations [2]. As the cost of percutaneous closure of ASD is reimbursed according to a specific diagnosis-related group, closing multiple ASDs with more than one device during a single procedure will exceed the diagnosis-related group budget.

When the defects are in close proximity, an attempt may be made to close all defects using a single device. Szkutnik et al. [6] reported the feasibility of this approach in 2004. A distance of less than 7 mm between defects is considered appropriate for this procedure, and a larger device should be employed to cover all the defects. In addition to the diameter of the device, a decision must be made regarding the type of device. A single regular ASD occluder inserted through the central or largest defect will be stabilized in place by its waist, which will also stretch the IAS, thereby bringing the surrounding defects in proximity and decreasing their size. The benefits of using a single device are a shorter procedure duration and less chance of interference with venous blood flow, atrioventricular valve function, or adjacent tissue erosion.

Balloon-Assisted Deployment of ASD Occluder

A 38-year-old female with a history of systemic lupus erythematosus was admitted for closure of a 15-mm secundum ASD associated with aneurysmat-

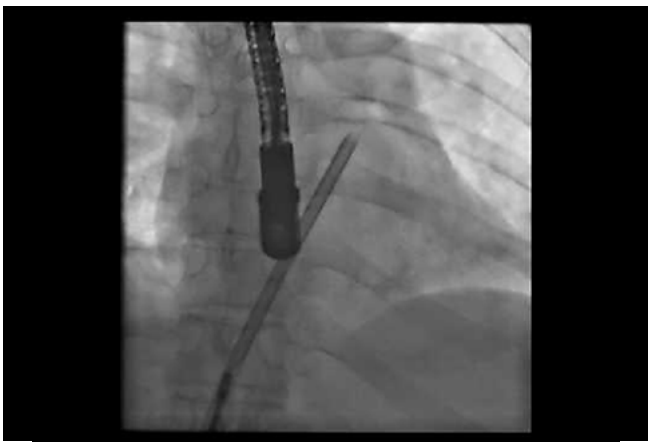

Video 1. The occluder was malaligned with the defect. View supplemental video at http://dx.doi.org/10.12945/j.jshd.2016.005.16.vid.01.

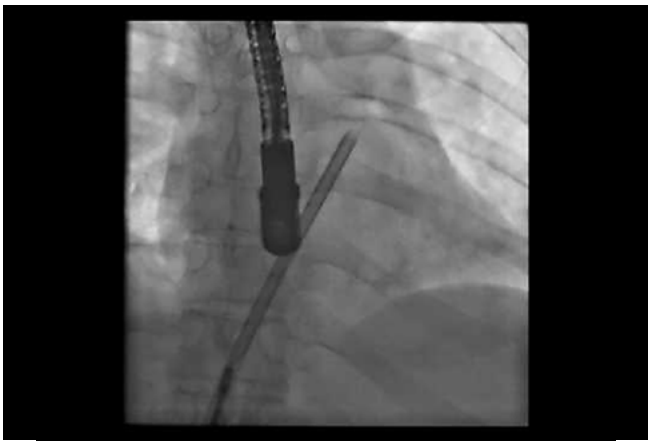

Video 3. The left disc is deployed and held in the left atrium by the balloon. The right disc was uncovered in the right atrium, engaging the interatrial septum. View supplemental video at http://dx.doi.org/10.12945/j.jshd.2016.005.16.vid.03.

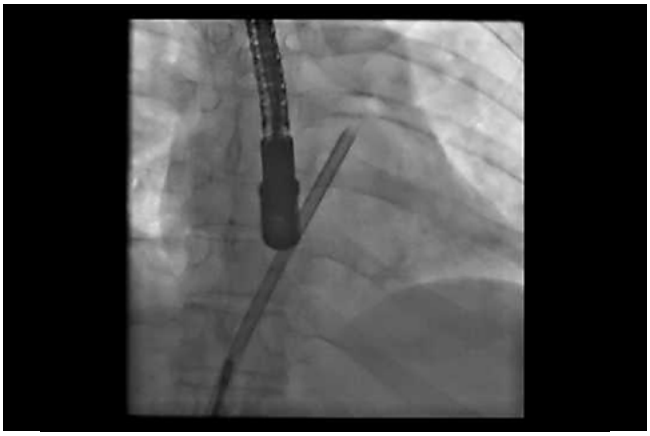

Video 2. The balloon was partially inflated in the defect. View supplemental video at http://dx.doi.org/10.12945/j.jshd.2016.005.16.vid.02.

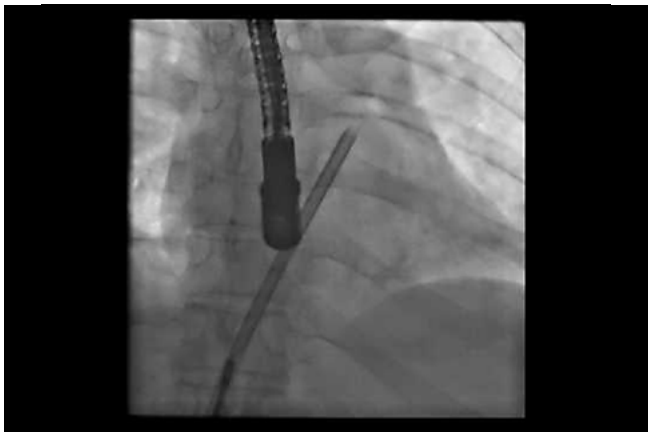

Video 4. Balloon deflation and retrieval while the left disc engaged the left aspect of the interatrial septum. View supplemental video at http://dx.doi.org/10.12945/j.jshd.2016.005.16.vid.04.

ic IAS. In the catheterization laboratory, the occluder failed to align properly with the defect, causing the left disc to be easily pulled through the ASD in repeated attempts of deployment (Video 1), including clockwise rotation of the sheath to allow initial deployment of the left atrial disc in the vicinity of the right upper pulmonary vein. To stabilize the device, a balloon was inserted through an additional femoral venous sheath and partially inflated in the left atrium (LA; Video 2). The left disc was then deployed and held in the LA by the balloon. While the left disc was anchored in the LA, the right disc was pulled and uncovered in the right atrium (RA) and then advanced toward the IAS, engaging it appropriately (Video 3). The balloon was deflated and carefully retrieved, allowing the left disc to approach the septum (Video 4). The guidewire was also slowly pulled back. The device remained in a suitable position following its release (Video 5).

The balloon-assisted technique can assist in the proper positioning of devices in difficult ASDs [7, 8]. In one case series, balloon-assisted device closure of large (≥35 mm) ASDs had a 90% success rate [9]. The balloon-assisted technique facilitates controlled delivery and device alignment in very large ASDs and is often helpful when conventional delivery fails.

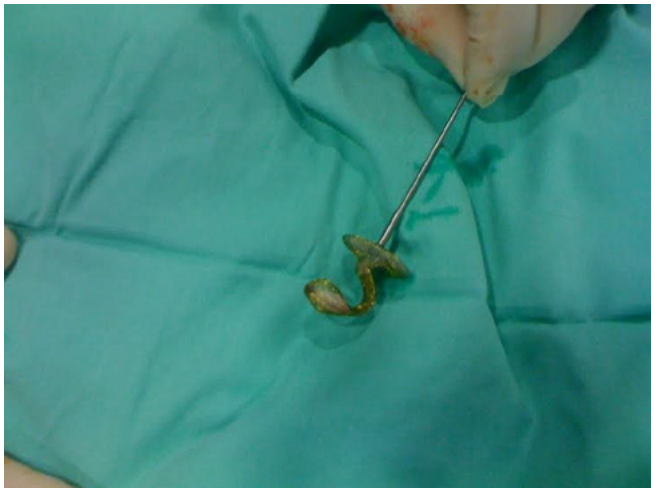

Figure 4. Extracted device.

Figure 5. Extracted device.

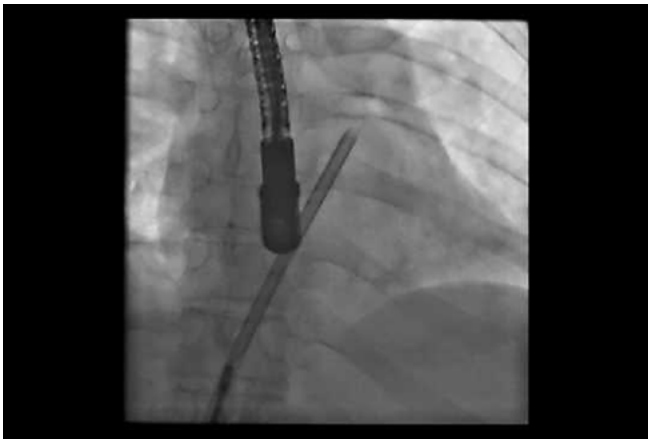

Video 5. The occluder was released and remained in position. View supplemental video at http://dx.doi.org/10.12945/j.jshd.2016.005.16.vid.05.

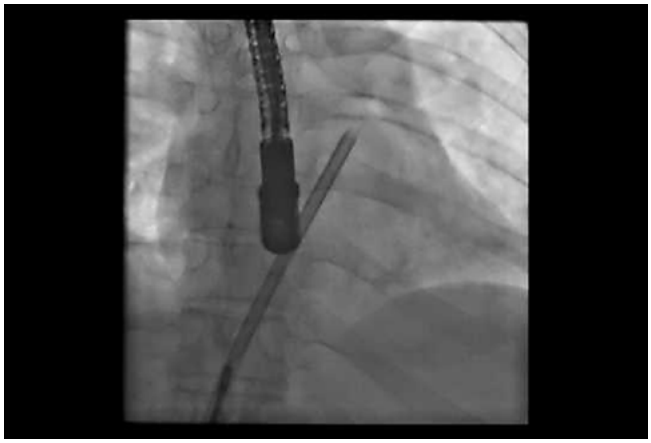

Video 6. A 32-mm atrial septal defect with reasonable margins. View supplemental video at http://dx.doi.org/10.12945/j.jshd.2016.005.16.vid.06.

Dilator-Assisted Deployment of ASD Occluder

A 62-year-old female was admitted for closure of a large secundum ASD causing exertional dyspnea. A 32-mm ASD with reasonable margins was measured by TEE (Video 6). The occluding device did not align appropriately with the IAS during multiple attempts (Videos 7 and 8). Therefore, the long dilator of the device delivery system was introduced over a J-wire through an additional venipuncture (Video 9). The dilator was used to retain the left disc in the LA as the right disc was uncovered and pulled gently toward the RA, allowing engagement of the IAS from the right aspect (Videos 10 and 11). This technique has also been shown to aid the closure of large ASDs when difficulties in proper deployment of the occlusive device are encountered [10, 11].

"Cobra"-Shaped Disfiguration of the Left Disc

During advancement of the septal occluder through the sheath, twisting or compression of the occluding device prohibited the left atrial disc from acquiring its proper "mushroom" shape, resulting in a "cobra"-shaped disfiguration (Video 12). The devices could not be deployed in this configuration and had to be removed and discarded (Figures 4 and 5). Previously published techniques using the Amplatzer septal occluder to overcome this "cobra"-like formation have included retrieving the device into the sheath

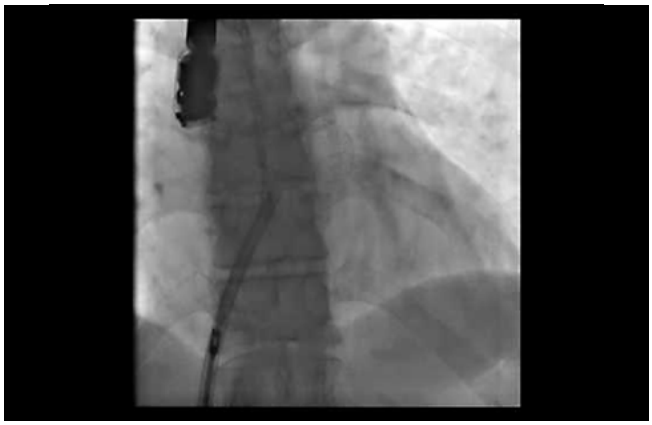

Video 7. The occluder failed to align appropriately with the interatrial septum. View supplemental video at http://dx.doi.org/10.12945/j.jshd.2016.005.16.vid.07.

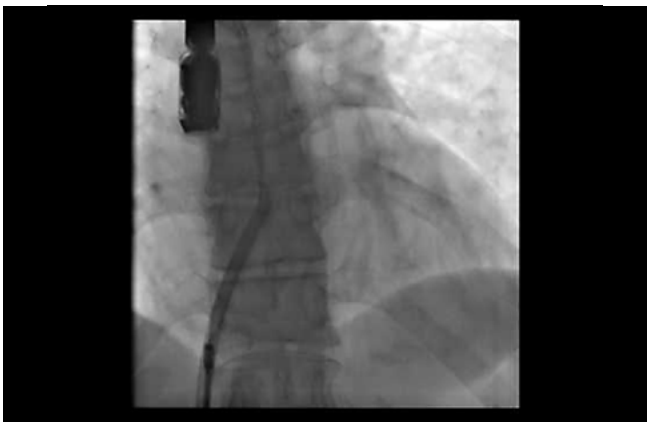

Video 8. Another failed attempt to align the occluder with the interatrial septum. View supplemental video at http://dx.doi.org/10.12945/j.jshd.2016.005.16.vid.08.

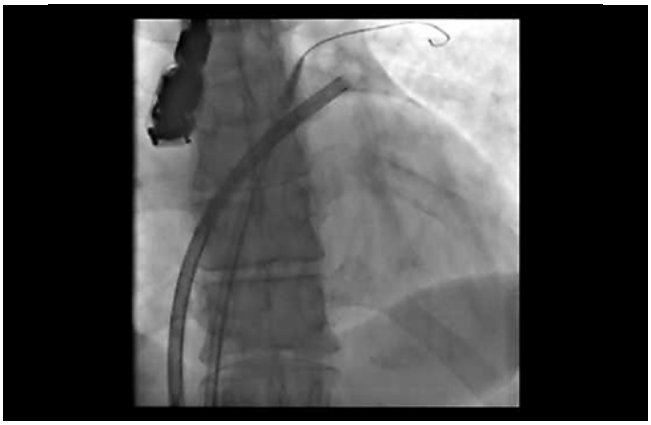

Video 9. The dilator was introduced to facilitate deployment. View supplemental video at http://dx.doi.org/10.12945/j.jshd.2016.005.16.vid.09.

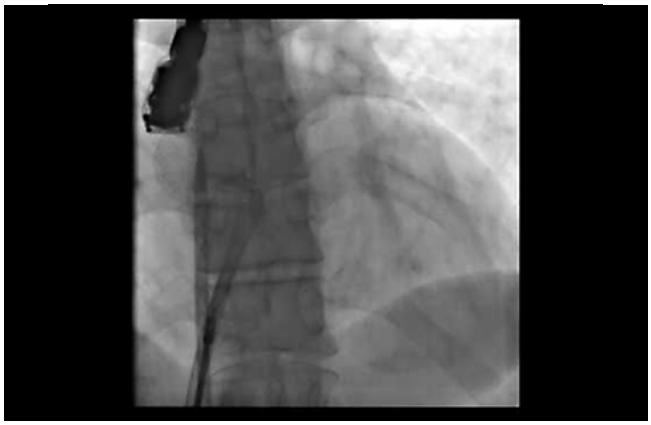

Video 10. The dilator retained the left disc in the left atrium, allowing engagement of the interatrial septum from the right. View supplemental video at http://dx.doi.org/10.12945/j.jshd.2016.005.16.vid.10.

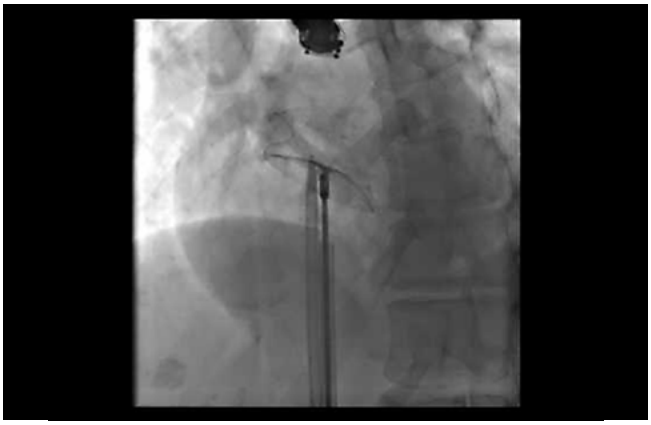

Video 11. After successful deployment the dilator is withdrawn. View supplemental video at http://dx.doi.org/10.12945/j.jshd.2016.005.16.vid.11.

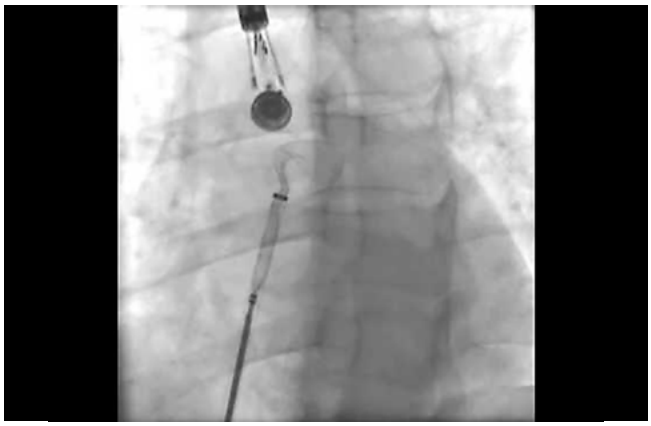

Video 12. "Cobra"-shape disfiguration of the left disc. View supplemental video at http://dx.doi.org/10.12945/j.jshd.2016.005.16.vid.12.

Video 13. Deploying the entire device in the left atrium allowed the device to return to its original shape. View supplemental video at http://dx.doi.org/10.12945/j.jshd.2016.005.16.vid.13.

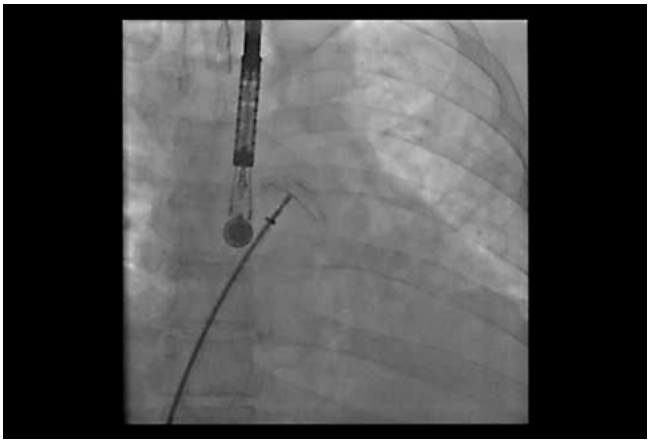

Video 14. Deploying the entire device in the left atrium allowed the device to return to its original shape. View supplemental video at http://dx.doi.org/10.12945/j.jshd.2016.005.16.vid.14.

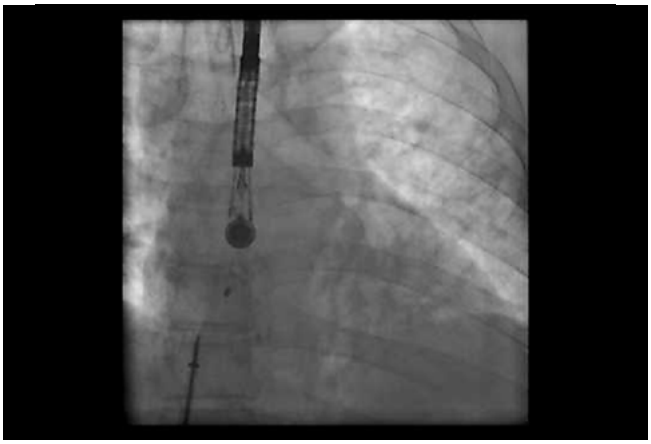

Video 15. Normal deployment and release of the device was possible. View supplemental video at http://dx.doi.org/10.12945/j.jshd.2016.005.16.vid.15.

and quickly redeploying the distal disc [12], repeating the procedure several times [13], and loading the device into the sheath while making back-and forth movements in the sheath [14]. Such attempts were at least partially effective in regaining normal device configuration. In our case, using the Occlutech device, we deployed the entire device in the LA (Video 13), allowing it to assume its original shape (Video 14). It was then possible to retrieve the right atrial disc and redeploy the device in the appropriate site with a normal configuration (Video 15). This technique may be effectively applied for all devices with "cobra"-like formations [15]. With the development of new technologies, however, this obstacle is less frequently encountered.

Deficient Aortic Rim

Deficient aortic rim is a rather common morphologic feature of ASD and is present in up to 30–50% of ASDs that are considered complex [16]. Deficient aortic rim is a risk factor for aortic erosion after device closure of ASDs. Deficient aortic rim has been associated with increased risk of device impingement on the aorta, but we observed no association between device impingement and the development of aortic insufficiency (Video 16). Ostermayer et al. found that small aortic rim is independently associated with procedural failure [17]. On the other hand, O'Byrne et al. found that deficient aortic rim is highly prevalent but does not seem to increase the risk of adverse outcomes [18]. Another group found that procedural failure mainly occurs with extremely large defects (≥40 mm), regardless of whether an aortic rim of septal tissue was present [19].

Absent aortic rim is not a contraindication for transcatheter closure attempt, but it may result in a more complex procedure and require maneuvers for successful deployment of the device. It is also important to consider whether to minimize the size of the device so that its edges/discs approach the aortic root or whether to select a slightly larger device that would embrace the aortic root to minimize the risk of aortic root erosion. These cases should be thoroughly investigated by TEE to demonstrate the extent of the aortic rim deficiency from several aspects, including 3-dimensional TEE. Adverse effects following an inter-

ventional closure of ASD in the presence of complex and extensively deficient aortic rim may occur not during the procedure but might become evident after the period of hospital stay. The complexity of the morphological anomaly should prompt questions about the safety and possible outcomes of the interventional procedure and the consideration of alternative surgical options that are safe and have a high likelihood of successful and uneventful outcomes. New technologies such as magnetic resonance imaging with 3-dimensional printing of a model representing the abnormal morphology may assist in decision-making in cases of complex anatomy.

Pulmonary Vein-Assisted Deployment of ASD Occluder

An asymptomatic 3-year-old boy was admitted for elective closure of a secundum ASD. TEE showed that the ASD measured 11 mm and had a deficient antero-superior aortic rim. In the catheterization laboratory, multiple attempts were made to achieve an adequate device position; however, the device slipped through the defect or resulted in a posture perpendicular to the defect (Video 17). To overcome this difficulty, we first deployed the right atrial disc and swiftly advanced it to the right aspect of the IAS, which allowed an optimal alignment of the left atrial disc with the IAS, occluding the defect. To delay the deployment of the left atrial disc, we started the deployment in the left upper pulmonary vein (LUPV). When the left disc was uncovered in the LUPV, we held it stationary in an elongated form, allowing unsheathing of the septal occluder so that the proximal disc would deploy in the RA, engaging the right aspect of the IAS. A short wiggle of the delivery system then released the left atrial disc from the LUPV position, engaging the IAS from the left aspect with a perfect configuration for ASD closure (Video 18). TEE investigation showed that the device embraced the aortic root and was in an adequate position in the presence of deficient aortic rim (Video 19). The pulmonary vein slide-out technique has also been used to aid closure of ASDs with deficient posterior rim [20]. This morphology is considered a risk factor for device migration.

Video 16. Atrial septal defect with deficient aortic rim with an occluder in situ embracing the aortic root. View supplemental video at http://dx.doi.org/10.12945/j.jshd.2016.005.16.vid.16.

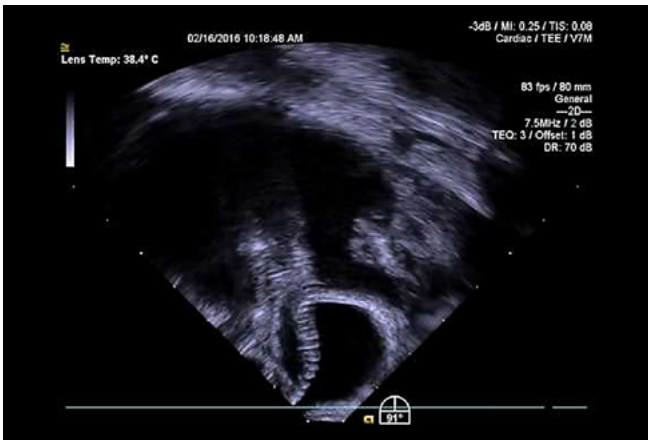

Video 17. The device was malaligned with the septum. View supplemental video at http://dx.doi.org/10.12945/j.jshd.2016.005.16.vid.17.

Video 18. The left disc was partially deployed in upper left pulmonary vein, allowing proper right disc deployment. View supplemental video at http://dx.doi.org/10.12945/j.jshd.2016.005.16.vid.18.

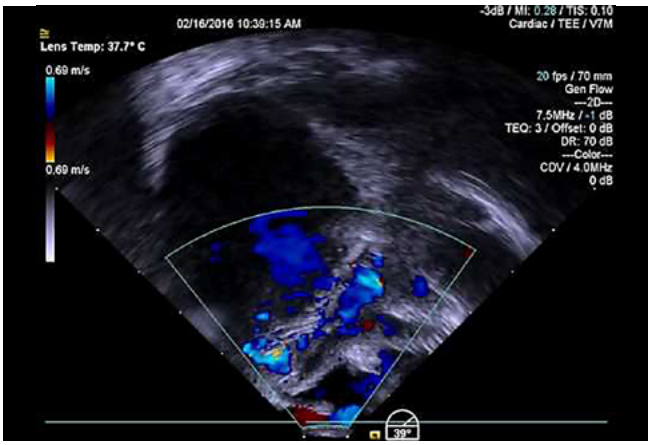

Video 19. The device assumed a normal position. View supplemental video at http://dx.doi.org/10.12945/j.jshd.2016.005.16.vid.19.

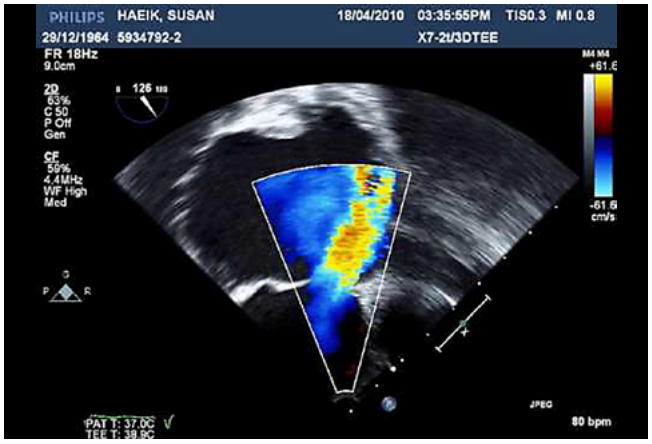

Video 20. Secundum atrial septal defect near the superior vena cava opening into the right atrium. View supplemental video at http://dx.doi.org/10.12945/j.jshd.2016.005.16.vid.20.

Video 21. Contrast injection in the superior vena cava confirmed no obstruction to superior vena cava flow. View supplemental video at http://dx.doi.org/10.12945/j.jshd.2016.005.16.vid.21.

"High" ASD

A "high"-positioned ASD, located in the postero-superior IAS, must be differentiated from sinus venosus defect, which may be described as the unroofing of right pulmonary veins into the superior vena cava (SVC) or the RA. Whereas sinus venosus defect cannot be closed by transcatheter intervention in the presence of partially anomalous pulmonary venous drainage, an attempt to close a high ASD can be made. Using TEE, we encountered an ASD in close proximity/continuity to the entrance of the SVC into the RA (Video 19). Occluding this ASD with a device carries a risk of restricting inflow from the SVC [21] and thrombus formation [22]. Therefore, during the procedure, after the device was deployed in the defect and prior to its release, contrast injection into the SVC in a steep left anterior oblique projection through an additional venous catheter demonstrated the spatial relationship between the SVC-RA junction and the occlusive device (Video 20) and showed unobstructed blood flow from the SVC to the RA (Video 21).

Large Chiari Network

The Chiari network is a fenestrated membrane consisting of threads and strands in the RA. It is a congenital remnant resulting from incomplete resorption of the right valve of the sinus venosus. Prominent Chiari network may be found in 2–3% of the population, but it is generally not of clinical importance. During transcatheter occlusion of ASD, the Chiari network can complicate the procedure by catheter entrapment [23], proximal disc entanglement and inadequate deployment [24], and residual shunt [25]. In our situation, the use of an additional catheter in the SVC was also helpful as in our previous case of "high" ASD. A catheter advanced from the femoral vein to the SVC may retain the Chiari network away from the IAS, thus lowering the probability of device or catheter entanglement.

Double Interatrial Septum

A 37-year-old patient with end-stage renal failure, who was awaiting renal transplantation from his wife, was referred for an elective percutaneous closure of

Video 22. Double interatrial septum. View supplemental video at http://dx.doi.org/10.12945/j.jshd.2016.005.16.vid.22.

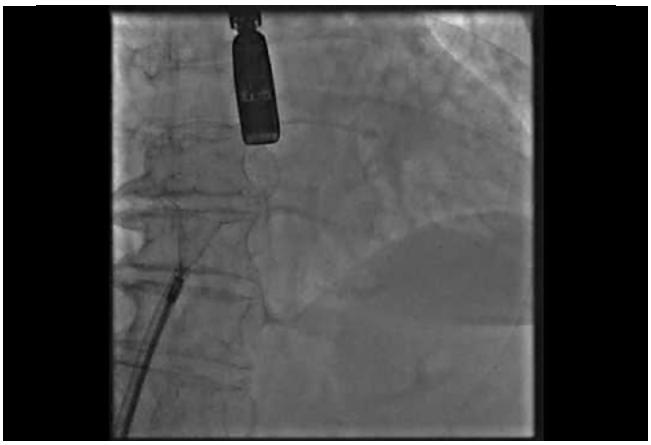

Video 23. Improper deployment of the entire device in the left atrium. View supplemental video at http://dx.doi.org/10.12945/j.jshd.2016.005.16.vid.23.

an ASD. The ASD was diagnosed incidentally on TTE while investigating atypical chest pain. The transplanting team demanded resolution of the cardiac anomaly prior to renal transplantation. Interestingly, there was a familial occurrence of ASD, as his father, three out of 10 siblings, and his son had previously undergone surgical repair of ASD. On TEE, marked RA and ventricular enlargement were noted, and an unusual morphology of the interatrial septum was encountered (Video 22). Two almost parallel ASDs were noted: a 23- × 28-mm defect in the normally located IAS and a 30-mm defect in the additional curtain located within the LA. The margins of the defects were quite flimsy. We observed normal pulmonary and systemic venous connections. No veins drained into the interatrial space formed between the double atrial septum. The atrial shunt was successfully closed with a single 38-mm Amplatzer ASO on first attempt. The distal disc was deployed in the LA distal to the accessory septum, whereas the proximal disc was deployed in the RA proximal to the normally located septum. Hence, the double atrial septum was fully approximated by the Amplatzer device. No residual shunt was noted during a 10-year follow-up period. The device had aligned well with the combined squashed septum. Percutaneous ASD closure in this patient was especially advantageous, as his end stage renal failure could critically complicate a surgical procedure.

Double atrial septum is an extremely rare atrial septal anomaly. It forms an interatrial space that usually communicates with the LA via a patent foramen ovale and with the RA via accessory atrial septal fenestration. These two passages are frequently formed at different levels, such as superior and inferior [26, 27]. Pulmonary veins may drain in the interatria l space; in this scenario, percutaneous ASD closure may occlude the drainage of this pulmonary vein. Surgical resection of the accessory atrial septum with ASD closure would be the appropriate approach. A pigtail catheter advanced into the right ventricle (RV) may aid in differentiating between double atrial septum and a prominent Eustachian valve; the diagnosis of double septum would be confirmed by a non-deflecting tissue, whereas a Eustachian valve would be drawn away by the catheter [28]. In our patient, we were able to pass the guide wire, the balloon sizing catheter, the delivery sheath, and subsequently the occluding device through both defects and also to achieve an adequate position and configuration of the device with optimal defect occlusion.

Snaring a Runaway Occluder

A 65-year-old woman with an ASD with deficient antero-superior rim and a floppy IAS underwent percutaneous closure of the ASD. Balloon-sizing of the defect measured 27 mm. A 30-mm Occlu-Tech septal occluder was selected. TEE inaccurately suggested an adequate deployment of the device

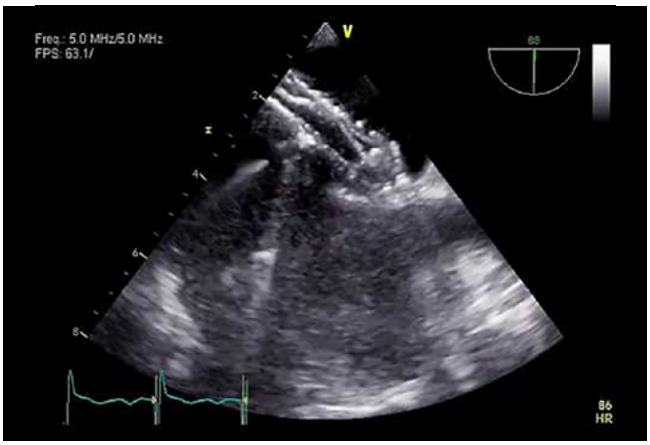

Video 24. "Cobra"-shape disfiguration of the left disc. View supplemental video at http://dx.doi.org/10.12945/j.jshd.2016.005.16.vid.24.

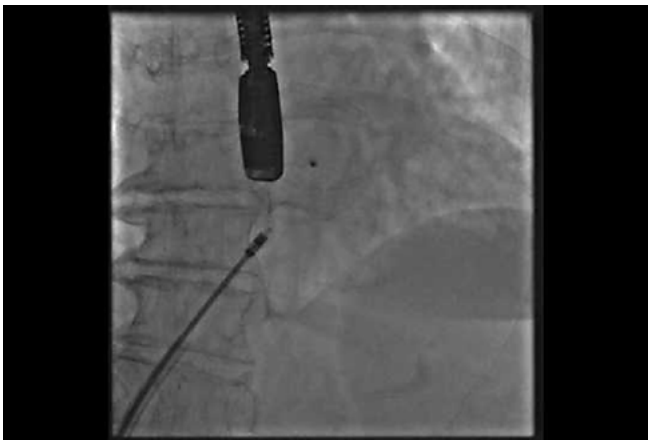

Video 25. A floating device in the left atrium following its release. View supplemental video at http://dx.doi.org/10.12945/j.jshd.2016.005.16.vid.25.

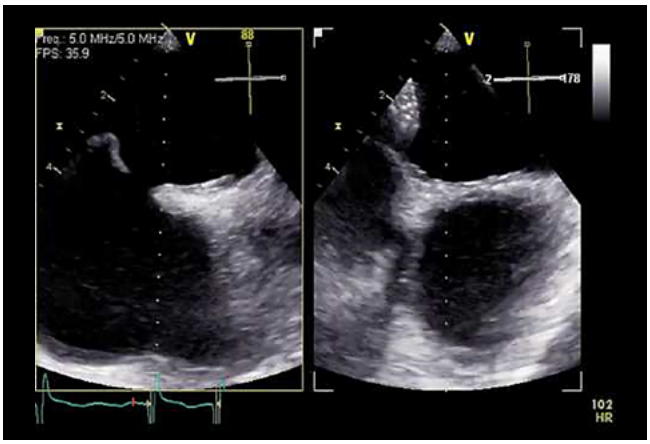

Video 26. A floating device in the left atrium following its release. View supplemental video at http://dx.doi.org/10.12945/j.jshd.2016.005.16.vid.26.

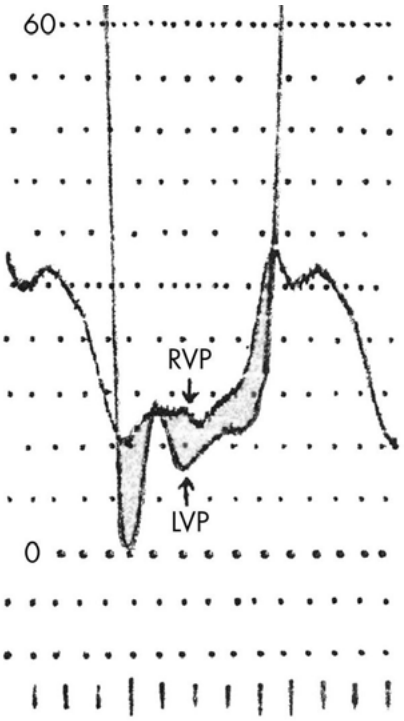

Figure 6. Simultaneous left ventricle (LV) and right ventricle (RV) pressure tracings during catheterization demonstrating higher diastolic pressure in the RV than in the LV.

(Videos 23 and 24). Following release, the device floated in the LA (Videos 25 and 26). The patient was given a supplement of heparin in addition to the initial dose. An attempt to retrieve the device with a 15-mm Andra snare failed. Although it was possible to hold on to the hub of the device, the grip was not strong enough to pull the device back into the 12F sheath (Video 27). Finally, the retention hub of the device was grabbed by 7F Cordis biopsy forceps (Video 28), allowing the right disc to be retrieved into the sheath (Video 29). The left disc was then approximated to the IAS, and the device was successfully deployed in the defect (Videos 30 and 31). The entire procedure was prolonged by 25 min. TTE confirmed an adequate position of the occluder the next day. In this scenario, attempting to recapture the connecting hub and accomplishing the procedure is desirable [29, 30]. Snaring and removing the device is another option. Emergent open-heart surgery is the last resort and should be reserved for unsuccessful device retrieval.

Video 27. Snaring attempts. View supplemental video at http://dx.doi.org/10.12945/j.jshd.2016.005.16.vid.27.

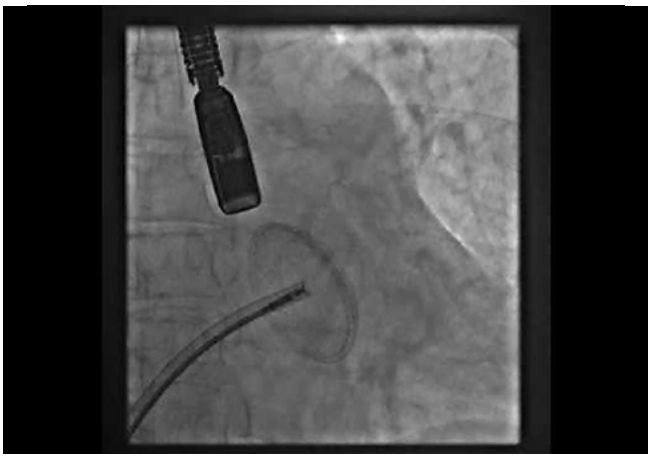

Video 29. The device was seized and retrieved by biopsy forceps. View supplemental video at http://dx.doi.org/10.12945/j.jshd.2016.005.16.vid.29.

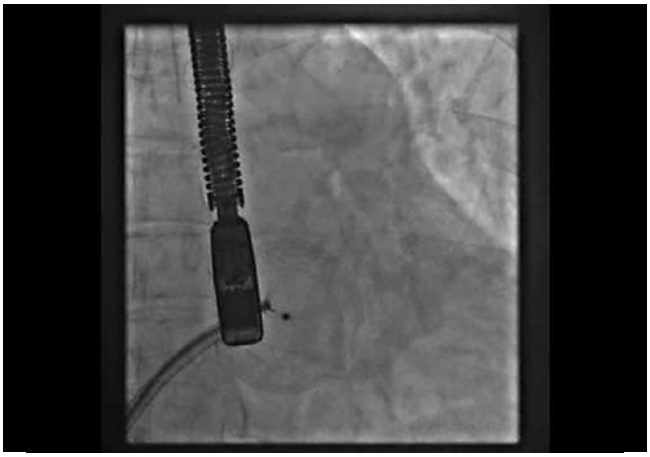

Video 28. The device was seized and retrieved by biopsy forceps. View supplemental video at http://dx.doi.org/10.12945/j.jshd.2016.005.16.vid.28.

Video 30. Re-deployment of the device. View supplemental video at http://dx.doi.org/10.12945/j.jshd.2016.005.16.vid.30.

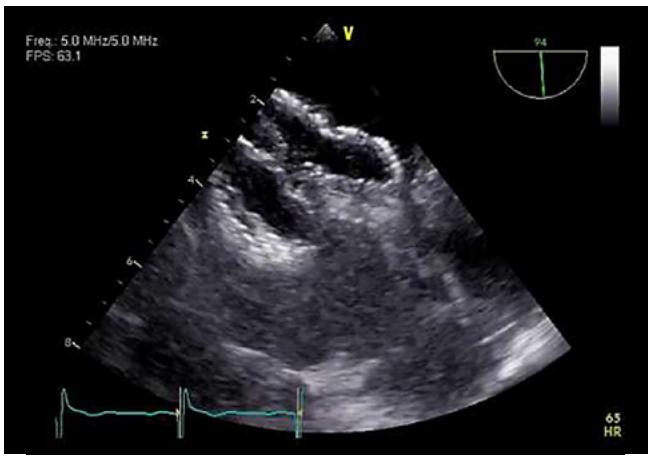

Video 31. Re-deployment of the device. View supplemental video at http://dx.doi.org/10.12945/j.jshd.2016.005.16.vid.31.

RV Diastolic Dysfunction Causing Cyanosis

A 73-year-old woman presented with profound central cyanosis and a history of minor stroke. She had normal heart morphology, normal pulmonary artery pressure, and normal coronary angiography. A massive right-to-left shunt was demonstrated at atrial level, with normal pulmonary venous saturations and PO2 values. The reason for this huge right-to-left shunt is illustrated by the diastolic pressure curves, representing compliance differences between the right and left ventricles (Figure 6). Other causes of atrial right-to-left shunt, including pulmonary disease, pulmonary vascular disease, RV hypertrophy, RV

systolic dysfunction, RA myxoma, tricuspid valve disease, and pericardial effusion, were excluded. Balloon occlusion of the patent foramen ovale served to test the tolerance of the occlusion and measure the effective stretched defect size. The defect was then closed by a 24-mm ASD Amplatzer occluder, resulting in a rise of arterial PO2 from 40 to 320 mmHg.

Atrial-level right-to-left shunt (ARLS) is a rare but important cause of hypoxia. The pathophysiology arises from an interatrial defect coupled with a secondary cardiac or pulmonary insult. A rise in RA pressure above LA pressure may precipitate ARLS [31]. Diastolic RV dysfunction may be caused by different mechanisms, including acute myocardial infarction, age-related undiagnosed severe pulmonary stenosis, and pulmonary atresia with intact interventricular septum years following resolution of RV outflow obstruction [32]. Treatment of ARLS involves treating the underlying cause and/or closure of the shunt to resolve hypoxemia. Observing the tolerance of a temporary closure of the ASD with a sizing balloon while monitoring RA pressure and systemic blood pressure should prevent RA pressure elevation and reduce cardiac output. If balloon occlusion is well-tolerated, the ASD (or patent foramen ovale) may be closed safely with a device and result in a favorable outcome.

Pulmonary arterial hypertension may also lead to ARLS in the presence of interatrial communication. However, prior to attempting to close an ASD in this situation, the reversibility of pulmonary hypertension should be demonstrated to avoid RV failure. A balloon occlusion test with RA pressure monitoring is a prudent approach. A fenestrated occluder may be considered as a temporary vent mechanism [33].

Summary

We present these select cases as challenges that require pre-procedural planning and intra-procedural considerations to successfully perform the percutaneous approach as an alternative to surgery without compromising patient safety. Some complex ASDs may be better treated by the surgeon, avoiding unpredictable percutaneous interventional outcome. Mature judgement and the acknowledgement of the current technology limitations is needed to hand over cases to the surgical team. However, the interventional team is expected to be resourceful in preparing for and performing the procedure. Learning from others' experience, as well as the prudent use of imaging modalities, personal experience, and proper selection of equipment, are beneficial when managing complex cases of ASD closure.

Conflict of Interest

The authors have no conflict of interest relevant to this publication.

References

1. Du ZD, Hijazi ZM, Kleinman CS, Silverman NH, Amplatzer investigators. Comparison between transcatheter and surgical closure of secundum atrial septal defect in children and adults: results of a multicenter nonrandomized trial. J Am Coll Cardiol. 2002;39:1836-1844. DOI: 10.1016/S0735-1097(02)01862-4
2. Tal R, Dahud Q, Lorber A. Fenestrated atrial septal defect percutaneously occluded by a single device: procedural and financial considerations. Cardiol Ther. 2013;2:97-102. DOI: 10.1007/s40119-012-0009-5
3. Awad SM, Garay FF, Cao QL, Hijazi ZM. Multiple Amplatzer septal occluder devices for multiple atrial communications: immediate and long-term follow-up results. Catheter Cardiovasc Interv. 2007;70:265-273. DOI: 10.1002/ccd.21145
4. Tillman T, Mulingtapang R, Sullebarger JT. Approach to percutaneous closure in patients with multiple atrial septal defects. J Invasive Cardiol. 2008;20:E167-E170. PMID: 18460721
5. Butera G, Romagnoli E, Saliba Z, et al. Percutaneous closure of multiple defects of the atrial septum: procedural results and long-term follow-up. Catheter Cardiovasc Interv. 2010;76:121-128. DOI: 10.1002/ccd.22435
6. Szkutnik M, Masura J, Bialikowski J, Gavora P, Banaszak P, Kusa J, et al. Transcatheter closure of double atrial septal defects with a single Amplatzer device. Catheter Cardiovasc Interv. 2004;61:237-241. DOI: 10.1002/ccd.10753
7. El Saiedi SA, Attia WA. New pediatric version of balloon-assisted technique for atrial septal defect closure using self-centering devices: Relation to interatrial septal thickness. J Invasive Cardiol. 2015;27:510-515. PMID: 26524205
8. Narin N, Baykan A, Argun M, Ozyurt A, Pamukcu O, Bayram A, et al. New modified balloon-assisted technique to provide appropriate deployment in the closure of large secundum atrial septal defect using amplatzer septal occluder in children. J Invasive Cardiol. 2014;26:597-602. PMID: 25364001
9. Pillai AA, Rangaswamy Balasubramanian V, Selvaraj R, Saktheeswaran M, Satheesh

S, Jayaraman B. Utility of balloon assisted technique in trans catheter closure of very large (≥35 mm) atrial septal defects. Cardiovasc Diagn Ther. 2014;4:21-27. DOI: 10.3978/j.issn.2223-3652.2014.02.05

10. Fu YC, Cao QL, Hijazi ZM. Device closure of large atrial septal defects: technical considerations. J Cardiovasc Med (Hagerstown). 2007;8:30-33. DOI: 10.2459/01.JCM.0000247432.74699.47
11. Wahab HA, Bairam AR, Cao QL, Hijazi ZM. Novel technique to prevent prolapse of the Amplatzer septal occluder through large atrial septal defect. Catheter Cardiovasc Interv. 2003;60:543-545. DOI: 10.1002/ccd.10686
12. Fischer G, Stieh J, Uebing A, et al. Experience with transcatheter closure of secundum atrial septal defects using the Amplatzer septal occlude: A single centre study in 236 consecutive patients. Heart. 2003;89:199-204. PMID: 12527678
13. Mazic U, Gavora P, Masura J. "Cobra-like" deformation of an Amplatzer septal occluder. Pediatr Cardiol. 2001;22:253-254. DOI: 10.1007/s002460010216
14. Estévez-Loureiro R, Martínez-Bendayan I, Salgado-Fernández J, Rueda-Núñez F. Cobra-like deformation of Amplatzer devices used for closing atrial septal defects: Can it be avoided? Rev Esp Cardiol. 2010;63:495-496. DOI: 10.1016/S1885-5857(10)70103-1
15. Aaron S, Mainzer G, Lorber A. Taming the "cobra": an approach to "cobra-like" formation seen in the Occlutech atrial septal defect and patent foramen ovale occluders. Catheter Cardiovasc Interv. 2012;79:678-680. DOI: 10.1002/ccd.23303
16. Pillai AA, Satheesh S, Pakkirisamy G, Selvaraj R, Jayaraman B. Techniques and outcomes of transcatheter closure of complex atrial septal defects - single center experience. Indian Heart J. 2014;66:38-44. DOI: 10.1016/j.ihj.2013.12.016
17. Ostermayer SH, Srivastava S, Doucette JT, Ko HH, Geiger M, Parness IA, et al. Malattached septum primum and deficient septal rim predict unsuccessful transcatheter closure of atrial communications. Catheter Cardiovasc Interv. 2015;86:1195-1203. DOI: 10.1002/ccd.26102.
18. O'Byrne ML, Glatz AC, Sunderji S, Mathew AE, Goldberg DJ, Dori Y, et al. Prevalence of deficient retro-aortic rim and its effects on outcomes in device closure of atrial septal defects. Pediatr Cardiol. 2014;35:1181-1190. DOI: 10.1007/s00246-014-0914-6.
19. Romanelli G, Harper RW, Mottram PM. Transcatheter closure of secundum atrial septal defects: results in patients with large and extreme defects. Heart Lung Circ. 2014;23:127-131. DOI: 10.1016/j.hlc.2013.07.020.
20. Papa M, Gaspardone A, Fragasso G, Sidoti F, Agricola E, Geoffrè G, et al. Feasibility and safety of transcatheter closure of atrial septal defects with deficient posterior rim. Catheter Cardiovasc Interv. 2013;81:1180-1187. DOI: 10.1002/ccd.24633.
21. Kahya Eren N, Kocabaş U, Nazlı C, Ergene O. Obstruction of superior vena cava flow during transcatheter atrial septal defect closure with the Atriasept ASD occluder. Turk Kardiyol Dern Ars. 2013;41:141-143. DOI: 10.5543/tkda.2013.95580.
22. Bijulal S, Sivasankaran S, Ajitkumar VK. An unusual thrombotic complication during percutaneous closure of atrial septal defect. J Invasive Cardiol. 2009;21:83-85.
23. Aydın A, Gürol T, Yılmazer MS, Dağdeviren B. Catheter entrapment around the Chiari network during percutaneous atrial septal defect closure. Anadolu Kardiyol Derg. 2011;11:E6-E7. DOI: 10.5152/akd.2011.047.
24. Cooke JC, Gelman JS, Harper RW. Chiari network entanglement and herniation into the left atrium by an atrial septal defect occluder device. J Am Soc Echocardiogr. 1999;12:601-603.
25. Greutmann M, Greutmann-Yantiri M, Kretschmar O, Senn O, Roffi M, Jenni R, et al. Percutaneous PFO closure with Amplatzer PFO occluder: predictors of residual shunts at 6 months follow-up. Congenit Heart Dis. 2009;4:252-257. DOI: 10.1111/j.1747-0803.2009.00302.x.
26. Kim IS, Jin MN, Song C, Kim YJ, Ji AY, Son JW, et al. The case of isolated double atrial septum with persistent interatrial space. J Cardiovasc Ultrasound. 2013;21:197-199. DOI: 10.4250/jcu.2013.21.4.197.
27. Roberson DA, Javois AJ, Cui W, Madronero LF, Cuneo BF, Muangmingsuk S. Double atrial septum with persistent interatrial space: echocardiographic features of a rare atrial septal malformation. J Am Soc Echocardiogr. 2006;19:1175-1181. DOI: 10.1016/j.echo.2006.04.001.
28. Freixa X, Regueiro A, Neves de Araujo G, Leal N, Sabaté M. Double atrial septum or redundant Eustachian valve: procedural management during atrial septal defect occlusion. EuroIntervention. 2015;11:e1-e2. DOI: 10.4244/EIJV11I6A141.
29. Peuster M, Boekenkamp R, Kaulitz R, Fink C, Hausdorf G. Transcatheter retrieval and repositioning of an Amplatzer device embolized into the left atrium. Catheter Cardiovasc Interv. 2000;51:297-300.
30. Ahn J, Kim JH, Choi JH, Oh JH. Percutaneous retrieval and redeployment of an atrial septal occluder under three-dimensional transesophageal echocardiographic guidance: a case report. J Korean Med Sci. 2014;29:871-873. DOI: 10.3346/jkms.2014.29.6.871.
31. Shnaider H, Shiran A, Lorber A. Right ventricular diastolic dysfunction and patent foramen ovale causing profound cyanosis. Heart. 2004;90:e31.
32. Gelernter-Yaniv L, Khoury A, Schwartz Y, Lorber A. Transcatheter closure of right-to-left interatrial shunts to resolve hypoxemia. Congenit Heart Dis. 2008;3:47-53. DOI: 10.1111/j.1747-0803.2007.00157.x.
33. Tal R, Schwartz Y, Lorber A. Staged approach for the management of ASD in presence of a small left ventricle and supra-systemic pulmonary pressure. Curr Res Cardiol. 2014;2:114-116.

Cite this article as: Tal R, Dotan M, Schwartz Y, Lorber A. Challenges in Atrial Septal Defect Occlusion. Structural Heart Disease. 2017;3(1):15-27. DOI: http://dx.doi.org/10.12945/j.jshd.2017.16.005

JSHD
Journal of Structural Heart Disease

Case Report

Journal of Structural Heart Disease, February 2017,
Volume 3, Issue 1:28-34
DOI: http://dx.doi.org/10.12945/j.jshd.2017.16.007

Received: May 10, 2016
Accepted: August 3, 2016
Published online: February 2017

Use of a Palmaz Intrahepatic Stent for Fixation of a CoreValve During Treatment of Native Aortic Valve Regurgitation

Nirmal Sunkara, MD[1*], Anwar Tandar, MD[1], Amit N. Patel, MD[1,2], Mary Hunt Martin, MD[1,2], Frederick Welt, MD[1]

[1] Division of Cardiovascular Medicine, University of Utah, Salt Lake City, Utah, USA

[2] Primary Children's Hospital, University of Utah, Salt Lake City, Utah, USA

Abstract

Transcatheter aortic valve replacement has been approved and is widely used in the USA for severe calcific aortic stenosis in the high risk inoperable patient. While not approved in patients with native aortic regurgitation (NAVR), there are numerous reports of its use in such patients who are not deemed acceptable surgical candidates. The technical challenges in the NAVR population include lack of fluoroscopic markings due to absence of annular or cusp calcification, increased risk of malpositioning and a risk of residual aortic regurgitation resulting in a high rate (18.8 percent) of need for second valve implantations [1].

Nevertheless, there are numerous reports of TAVR for NAVR. Roy et.al in a registry study of 43 patients from 14 different countries showed feasibility of CoreValve implantation in extreme operative risk patients with NAVR without aortic stenosis [1]. The implantation of a CoreValve was successful in 97.7% of cases, however the Valve Academic Research Consortium (VARC)-defined procedural success was only 74.4% due to the need for a second valve.

We submit the first description of using the radial force of a Palmaz biliary stent to affix the upper portion of a CoreValve and mitigate the issue of ventricular migration of the valve in treatment of a NAVR patient with TAVR. We feel this should be considered as an additional tool in the armamentarium of physicians treating this challenging subset of patients.

The Palmaz XL stents are balloon expandable stainless steel prostheses. They have a closed cell design which gives them high radial strength and are designed for an expansion range of 10 mm – 25 mm while maintaining their radial strength of 12 psi. Their foreshortening ranges between 2.5% at 10 mm and 23% at 25 mm [4]. This foreshortening has to be taken into account when adjusting the overlap portion when using as described above with the CoreValve.

Key Words

Aortic regurgitation • TAVR • Core valve • Palmaz stent

Introduction

Transcatheter aortic valve replacement (TAVR) has been approved and is widely used in the United States for severe calcific aortic stenosis in high-risk inoperable patients. Although not approved for patients with native aortic regurgitation (NAVR), there are several reports of its use in such patients who are not deemed acceptable surgical candidates. Patients with NAVR pose numerous technical challenges. The absence of annular or cusp calcification in NAVR means a lack of fluoroscopic markings, which can make valve positioning more challenging. The lack of

Fax +1 203 785 3346
E-Mail: jshd@scienceinternational.org
http://structuralheartdisease.org/

ISSN 2326-4004

Accessible online at:
http://structuralheartdisease.org/

* Corresponding Author:
Nirmal T. Sunkara, MD
Division of Cardiovascular Medicine
University of Utah
30 N 1900 E, #4A100, Salt Lake City, UT 84101, USA
Tel. +1 657 333 2079, Fax: +1 888 433 9843, E-Mail: nirmalsunkara@gmail.com

a calcified substrate also increases the risk of malpositioning. Furthermore, there is a risk of residual aortic regurgitation, resulting in a high rate (18.8%) of need for second valve implantations [1].

Nevertheless, several reports have described the use of TAVR in patients with NAVR. In a registry study of 43 patients from 14 different countries, Roy et al. demonstrated the feasibility of CoreValve implantation in extreme operative risk patients with NAVR without aortic stenosis [1]. The implantation of a CoreValve was successful in 97.7% of cases; however, the Valve Academic Research Consortium-defined procedural success rate was only 74.4% due to the need for a second valve in some cases. The Italian CoreValve multicenter registry confirmed its feasibility in 26 patients and showed that patients with NAVR are usually younger than those undergoing TAVR for aortic stenosis [2]. In this report, we describe a challenging case of implanting a CoreValve for NAVR and a reproducible solution.

Case Presentation

The patient was a 38-year-old male with pulmonary valve dysplasia associated with Noonan's syndrome and hypertrophic cardiomyopathy. The patient underwent pulmonary valvotomy and myomectomy at 17 months of age followed by a pulmonary homograft for severe pulmonary insufficiency at 20 years of age. With a history of multiple episodes of infective endocarditis on the aortic valve, he subsequently developed severe aortic insufficiency and was referred to us for possible TAVR. Due to significant frailty, poor pulmonary function, and prior sternotomies, he was considered a candidate for TAVR. His STS score for mortality or morbidity was calculated as 24.83%.

Computed tomography (CT) measurements suggested a minimum annulus diameter of 23.3 mm and a maximum annulus diameter of 30.1 mm. The perimeter of the annulus was measured on CT images as 88 mm, and the area was calculated as 596.2 mm^2 (Figure 1). No calcification was noted in the annulus. Plans were made for implantation of a 31-mm CoreValve (Medtronic, Minneapolis, MN, USA).

The procedure was completed under general anesthesia. Transesophageal echo image guidance was used throughout the procedure. Bilateral femoral

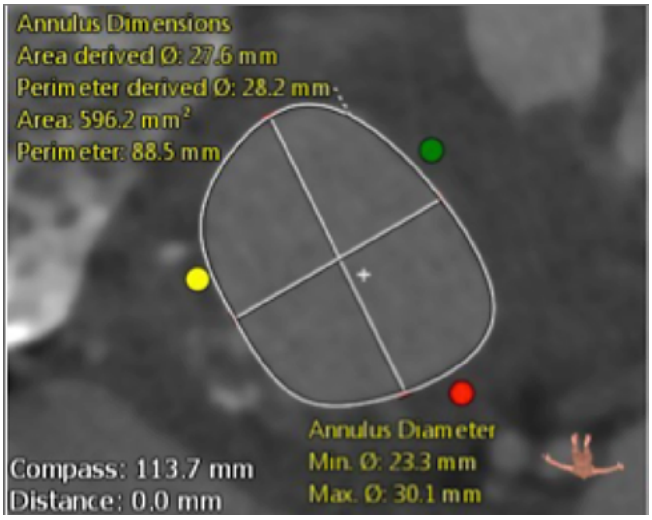

Figure 1. Aortic annulus measurements pre procedure using 3mensio showed a annulus perimeter of 88 mm and a maximum diameter of 30.1mm and a minimum diameter of 23.3 mm.

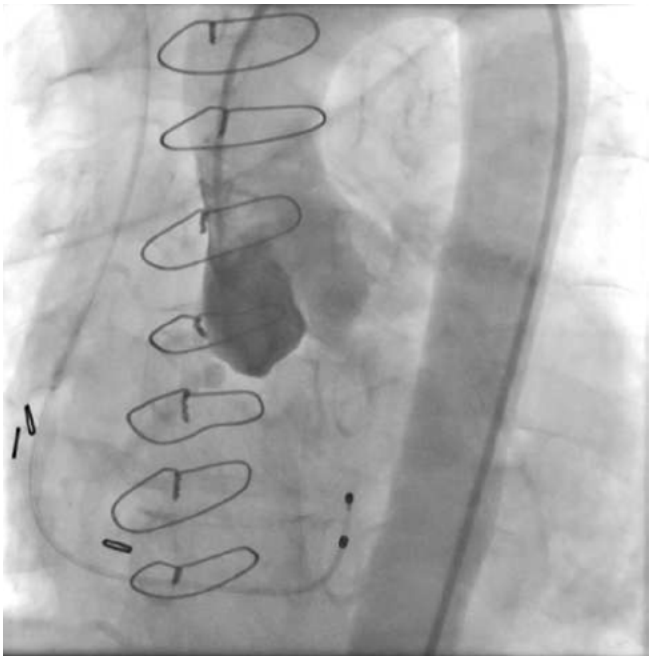

Figure 2. A 6-F pigtail catheter in the right coronary cusp.

artery access was obtained using a micropuncture needle and the modified Seldinger technique. A 6-F arterial sheath was placed in the left femoral artery, and a 6-F pigtail catheter was advanced over a 0.035 J wire and positioned in the right coronary aortic cusp (Figure 2). A 28-cm 18-F Gore dryseal sheath (Gore Medical, Flagstaff, AZ, USA) was placed in the right femoral artery. A double curve Lunderquist extra stiff

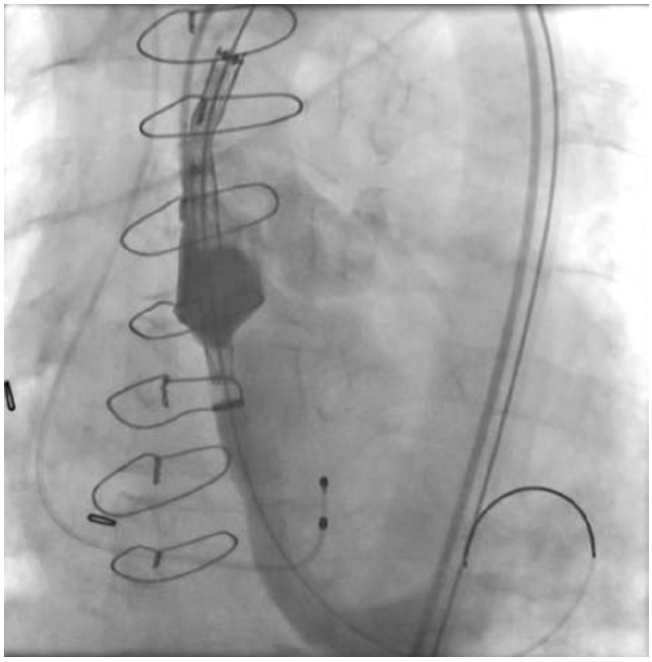

Figure 3. Appropriate positioning of the CoreValve pre-deployment.

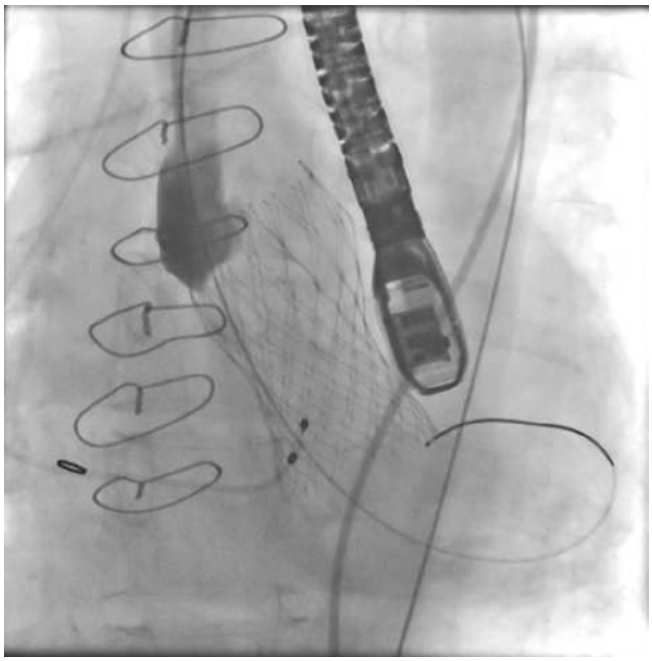

Figure 4. Deformation of the proximal struts of CoreValve suggesting external impingement. Ventricular displacement of the CoreValve is seen.

wire (Cook Medical, Bloomington, IN, USA) was positioned in the left ventricle to facilitate the CoreValve implantation.

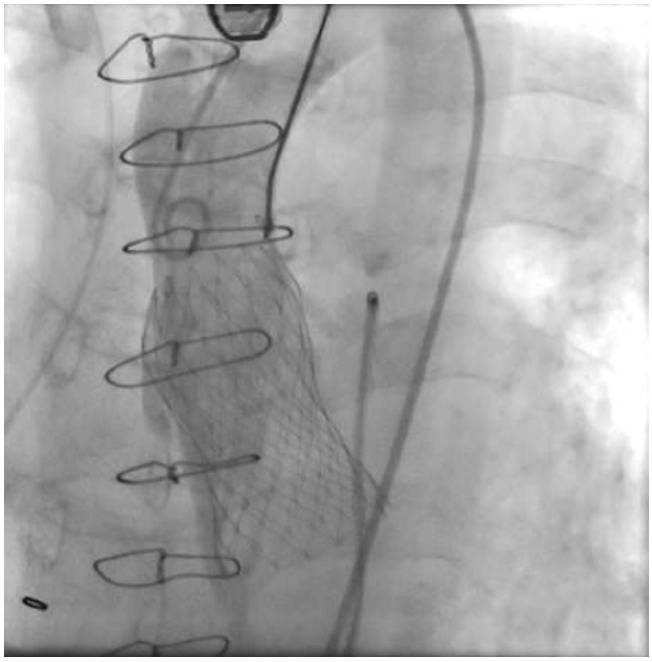

Figure 5. Left tab of the CoreValve snared with a 25-mm Amplatz GooseNeck snare and valve pulled into proper position. Note abluminal projection of the proximal struts.

A 31-mm CoreValve was prepped, and its orientation was confirmed. The valve was advanced across the aortic valve, confirming its position in the right coronary cusp using the pigtail catheter in coplanar view under fluoroscopy, and deployed under rapid pacing at 130 bpm. After valve deployment and release, it was noted to be functioning well initially but with impingement on the valve at the greater curvature of the aorta, which was thought to possibly be secondary to pulmonary artery enlargement (Figure 3). Subsequently, the valve migrated toward the ventricle in an unacceptably low position (Figure 3). Left radial arterial access was obtained, and a 120-cm 6-F GooseNeck snare (ev3, Amplatz, Plymouth, MN, USA), was advanced into the ascending aorta. The left tab of the valve oriented toward the lesser curvature of the aorta was snared with the 25-mm snare, and the valve was pulled cephalad into an appropriate position. However, with release of tension on the snare, the valve migrated toward the ventricle, which was thought to be due to impingement on the greater curvature of the aorta (Figure 4). CT measurements of the aorta at this level of impingement were approximately 23 mm × 20 mm.

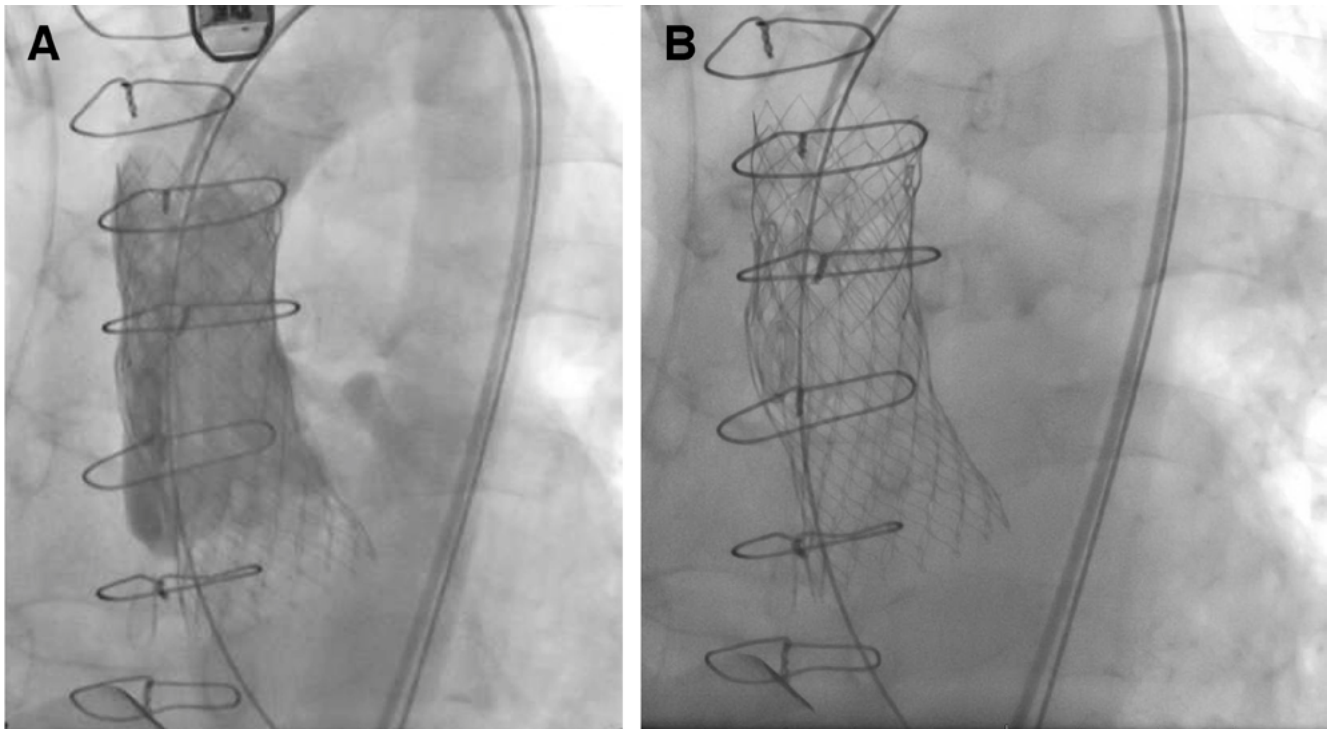

Figure 6. *Panel A*. CoreValve in appropriate position and patent coronary arteries with mild paravalvular leak noted on final aortogram. *Panel B*. CoreValve in appropriate position with the Palmaz XL deployed fixing the upper portion of the CoreValve.

To maintain the position of the valve, a Palmaz XL transhepatic biliary stent (40 mm unexpanded length × 10 mm expansion diameter; Cordis Corp., Rancho Cordova, CA, USA) was placed to achieve adequate radial force against the impingement. This Palmaz stent was then crimped onto a 24-mm balloon in balloon (BIB) catheter (inner: 12 mm diameter × 3 cm length, outer: 24-mm diameter × 4-cm length; NuMED Inc, Hopkinton, NY, USA). The outer balloon was then slightly inflated to prevent the Palmaz stent from sliding off the balloon. A 75-cm 12-F Check-Flo introducer sheath (Cook Medical, Bloomington, IN, USA) was used to advance the BIB balloon-mounted crimped Palmaz stent into the ascending aorta. The Check-Flo introducer sheath was then withdrawn, leaving the BIB balloon-mounted Palmaz stent in place overlapping the proximal stent end of the CoreValve. Rapid pacing at 180 bpm was initiated, and the inner and outer balloons were inflated in succession, securing the stent and valve in place, and the GooseNeck snare was released (Figure 5). The BIB balloon was then fully inflated to position the Palmaz stent, which appeared to fix the CoreValve in place. Post-procedure aortogram confirmed acceptable location of the valve, patency of the coronary arteries, and mild paravalvular leak (Figure 6). The patient was extubated immediately and monitored overnight in the intensive care unit. He felt symptomatically improved and was discharged home next day.

The patient showed a significant reduction in shortness of breath two weeks post-procedure and at 1-month follow-up. Echocardiographic evaluation at 2 and 6 months confirmed accurate positioning of the valve with good valve function (Figure 7A and 7B). However, we also noted moderate perivalvular regurgitation, highlighting difficulty in treating NAVR with TAVR. Furthermore, the 6-month follow-up echocardiogram revealed a moderate to severe paravalvular leak, and the patient exhibited increased fatigue and failure to thrive. After discussion, we decided to proceed with placing a valve-in-valve transcatheter using an overexpanded Sapien S3.

Discussion

This is the first description of the use of the radial force of a Palmaz biliary stent to affix the upper portion of a CoreValve and mitigate the ventricular mi-

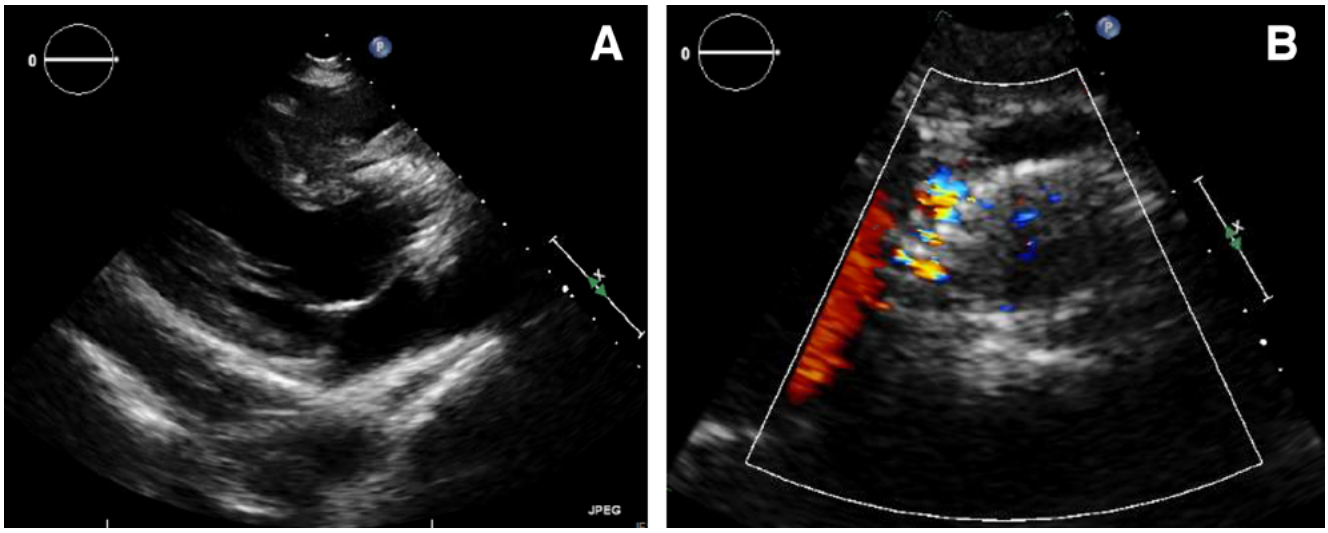

Figure 7. *Panel A*. Six-month follow-up transesophageal echocardiogram shows adequate positioning of the CoreValve in a parasternal long axis view. *Panel B*. Transesophageal echocardiogram short axis view of aortic valve showing turbulent flow suggestive of perivalvular leak.

gration of the valve in treating a NAVR patient with TAVR. We believe that this should be considered as a possible approach to treatment in this challenging subset of patients.

The CoreValve system consists of a self-expandable, tri-level frame made of nitinol attached to a tri-leaflet porcine pericardium heart valve. Most reports of TAVR for NAVR have utilized the CoreValve for its unique self-expanding properties. The upper third/outflow portion of the frame exerts low radial force and sits within the ascending aorta, functioning to orient the prosthesis in the direction of the aortic root and blood flow. The middle third of the frame is constrained to avoid jailing of the coronary arteries and hosts the valve leaflets. It has high hoop force to resist deformation and thus maintain normal leaflet function. The lower third/inflow portion of the frame sits within the left ventricular outflow tract/annulus of the native aortic valve and exerts high radial force. Thus, the prosthesis is anchored within the annulus, and its function is supra-annular [3, 4]. In our case, we required additional stabilization at the upper third/outflow portion of the valve, which was adequately provided by the Palmaz stent.

Palmaz stents are balloon-expandable stainless steel prostheses. All Palmaz stents have a closed cell design, which gives them high radial strength and makes them useful for treating coarctation of the aorta. Most Palmaz stents must be hand-crimped onto a balloon (for example, the 3010 is available mounted on a 12-mm delivery balloon). In the Palmaz stent nomenclature, first two digits indicate the unexpanded stent length, and the last one or two digits indicate the minimum recommended expansion diameter. Large Palmaz stents (P308) have a recommended expansion diameter between 8–12 mm, with reported overdilation to 18–20 mm. Overdilation of these stents leads to significant foreshortening <33% at 12 mm and up to 50% at 18 mm and decreases radial strength. Palmaz XL transhepatic stents are designed for an expansion range of 10–25 mm while maintaining a radial strength of 12 psi (comparative radial strength of the large Palmaz P308 stent is 6 psi). Their foreshortening ranges between 2.5% at 10 mm and 23% at 25 mm 10–13. In our situation, based on measurements of the ascending aorta and the root, both on CT prior to the procedure and aortogram during the procedure, we required a stent expanded to 23 mm. This required the use of a Palmaz XL transhepatic stent and a 1:1-sized balloon. The foreshortening of the Palmaz stent must be taken into account when determining the length of the stent to ensure adequate overlap with the CoreValve and to prevent jailing of the origin of the innominate and left carotid and subclavian arteries. We used a P4010 stent, accounting for foreshortening and the distance from

the origin of the innominate artery, to avoid jailing of this artery.

When choosing a balloon, diameter and length are important considerations. Shorter balloons offer the advantage of inflating the inner part of the stent first, thus avoiding the potential complication of flaring of the ends of the stents, resulting in balloon rupture or vessel wall perforation; however, this can result in stent sliding or embolization. Longer balloons allow more precise placement and repositioning if necessary before their full inflation. The BIB balloon has two balloons, one shorter (inner) and one longer (outer) than the stent, which offers potential advantages. In our situation, to prevent the crimped Palmaz stent from sliding off the balloon during its introduction into the sheath, we inflated the inner balloon to a low 2 atm. Once the sheath is withdrawn and the stent is adequately positioned, the inner balloon is inflated first. After the position of the inner balloon is ensured to be satisfactory, the outer balloon is inflated. In choosing the diameter of the balloon, we took into consideration the measurements of the ascending aorta based on pre-procedure CT and aortogram performed during the procedure. The balloon was sized 1:1 with the intent to expand the Palmaz stent and adequately fix the CoreValve in place.

Potential risks of this approach that should be kept in mind are vessel wall perforation while deploying the Palmaz stent, balloon rupture and aortic dissection, inadequate expansion of the Palmaz stent with ventricular migration of the stent and valve, and possible jailing of the major branches of aorta. Careful measurements of the ascending aorta and balloon and stent sizing, taking foreshortening into account, should minimize such complications.

There are a variety of other valves in various stages of development that are designed for the treatment of NAVR. These typically utilize a transapical approach and include the Acurate TA valve, Medtronic engager valve, and Jena valve [5-8]. The Helio transcatheter dock (Edwards Lifesciences, Irvine, CA, USA) has been described as an ancillary device intended to confer greater annular stability to the Edwards SAPIEN XT valve. The dock consists of a self-expandable nitinol stent with a polyethylene skirt designed to be positioned inside the aortic root, which is intended to secure the balloon-expandable SAPIEN XT by incorporating and entrapping the native cusps [9].

TAVR is not an approved treatment for NAVR, although it is being used off-label in high-risk surgical candidates. Experience in using the transcatheter approach to treat NAVR is limited but growing. Patients with mixed aortic valve disease with severe stenosis and at least moderate regurgitation have been successfully treated with both commercially available TAVR devices, but NAVR without stenosis is still considered a relative contraindication in published guidelines.

Newer-generation valve designs that use leaflet pinning or stabilization mechanisms are showing promise, but experience with these devices is still limited. Therefore, additional experience and evidence from larger registries, longer follow-up periods, and randomized clinical trials is necessary for the expanded use of TAVR for NAVR.

Conflict of Interest

Dr. Welt has reported as being on the advisory board for Medtronic.

Comment on this Article or Ask a Question

References

1. Roy DA, Schaefer U, Guetta V, Hildick-Smith D, Möllmann H, Dumonteil N, et al. Transcatheter aortic valve implantation for pure severe native aortic valve regurgitation. J Am Coll Cardiol. 2013;61:1577-1584. DOI: 10.1016/j.jacc.2013.01.018
2. Testa L, Latib A, Rossi ML, De Marco F, De Carlo M, Fiorina C, et al. CoreValve implantation for severe aortic regurgitation: a multicentre registry. EuroIntervention. 2014;10:739-745. DOI: 10.4244/EIJV10I6A127
3. Piazza N, de Jaegere P, Schultz C, Becker AE, Serruys PW, Anderson RH. Anatomy of the aortic valvar complex and its implications for transcatheter implantation of the aortic valve. Circ Cardiovasc Interv. 2008;1:74-81. DOI: 10.1161/CIRCINTERVENTIONS.108.780858
4. Adams DH, Popma JJ, Reardon MJ. Transcatheter aortic-valve replacement with a self-expanding prosthesis. N Engl J Med. 2014;371:1790-1798. DOI: 10.1056/NEJMc1408396
5. Seiffert M, Diemert P, Koschyk D, Schirmer J, Conradi L, Schnabel R, et al. Transapical implantation of a second-generation transcatheter heart valve in patients with noncalcified aortic regurgitation. JACC Cardiovasc Interv. 2013;6:590-597. DOI: 10.1016/j.

jcin.2013.01.138

6. Kiefer P, Seeburger J, Mohr FW, Holzhey DM. Transcatheter aortic valve replacement for isolated aortic valve insufficiency: experience with the Engager valve. J Thorac Cardiovasc Surg. 2014;147:e37-e38. DOI: 10.1016/j.jtcvs.2013.11.035
7. Sündermann SH, Holzhey D, Bleiziffer S, Treede H, Jacobs S, Falk V. Second-generation transapical valves: the Medtronic Engager system. Multimed Man Cardiothorac Surg. 2014;mmu001. DOI: 10.1093/mmcts/mmu001
8. Wendt D, Kahlert P, Pasa S, El-Chilali K, Al-Rashid F, Tsagakis K, et al. Transapical transcatheter aortic valve for severe aortic regurgitation: expanding the limits. JACC Cardiovasc Interv. 2014;7:1159-1167. DOI: 10.1016/j.jcin.2014.04.016
9. Barbanti M, Ye J, Pasupati S, El-Gamel A, Webb JG. The Helio transcatheter aortic dock for patients with aortic regurgitation. EuroIntervention. 2013;9 Suppl:S91-S94. DOI: 10.4244/EIJV9SSA17
10. Ebeid M. Balloon expandable stents for coarctation of the aorta: review of current status and technical considerations. Images Paediatr Cardiol. 2003;5:25-41. PMCID: PMC3232539
11. Peters B, Ewert P, Berger F. The role of stents in the treatment of congenital heart disease: Current status and future perspectives. Ann Pediatr Cardiol. 2009;2:3-23. DOI: 10.4103/0974-2069.52802
12. Forbes TJ, Gowda ST. Intravascular stent therapy for coarctation of the aorta. Methodist Debakey Cardiovasc J. 2014;10:82-87. PMID: 25114759
13. Montague BJ, Kakimoto WM, Arepally A, Razavi M, Dake MD, Hofmann, LV. Response of balloon-expandable endoprosthetic metallic stents subjected to over-expansion in vitro. Cardiovasc Intervent Radiol. 2004;27:158-163. DOI: 10.1007/s00270-003-4600-y

Cite this article as: Sunkara N, Tandar A, Patel AN, Martin MH, Welt F. Use of a Palmaz Intrahepatic Stent for Fixation of a CoreValve During Treatment of Native Aortic Valve Regurgitation. Structural Heart Disease. 2017;3(1):28-34. DOI: http://dx.doi.org/10.12945/j.jshd.2017.16.007